Reconstruction of Holocene Relative Sea-Level Positions for the Morgan Peninsula and Gulf Shores Area of Alabama Using Ground-Penetrating Radar

By

Andrew Robert Philbin

B.S. Texas A&M University, 2014

Submitted for the graduate degree program in the Department of Geology and Graduate Faculty of the University of Kansas in partial fulfillment of the requirements for the degree of Master of Science

_____

Chair: Michael Blum

_____

Georgios Tsoflias

_____

William Johnson

Thesis Defense May 7, 2020

The thesis committee for Andrew Philbin certifies that this is the approved version of the following thesis:

Reconstruction of Holocene Relative Sea-Level Positions for the Morgan Peninsula and Gulf Shores Area of Alabama Using Ground-Penetrating Radar

_____

Chair: Michael Blum

Date Approved: 7 May 2020

Abstract

Holocene sea-level rise along the northern Gulf of Mexico coast has been debated. One hypothesis interprets basal peats from the Mississippi Delta to indicate continual sea-level rise for the Gulf of Mexico. An alternate hypothesis proposes that data from the subsiding delta is primarily a subsidence signal, and that sandy non-deltaic shorelines indicate that regional sea level reached present elevations by the mid-to-late Holocene, with minor oscillations since then. This research focuses on utilizing Holocene progradational sandy shorelines of the Morgan Peninsula in the eastern Gulf of Mexico as sea-level indicators. Sandy shorelines in this area are ideal to examine sea level change because they are well preserved, sufficiently distant from the subsiding delta, well mapped, and numerically dated by previous studies.

To document Holocene sea level change, two-dimensional ground-penetrating radar imaging of well-dated beach-ridge successions is used to identify changes in the elevation of the shoreface clinoform topset-foreset-break through time. The topset- foreset break is observed in GPR imaging of the modern Morgan Peninsula shoreline and represents the transition between flat-lying foreshore and seaward-dipping shoreface facies. Because the topset-foreset-break occurs in the modern intertidal zone, relict topset-foreset-breaks observed in beach ridge successions are reliable sea-level indicators.

Beach-ridge successions with optical luminescence (OSL) ages of 5.5 ka display topset-foreset breaks at -0.545 m below mean sea level. Topset-foreset-breaks occur at 0.075 m above mean sea level in beach-ridge successions from 3.5 ka and reach a maximum elevation of 0.205 m above mean sea level at 2.4 ka. These data support the view that current sea-level in the Morgan Peninsula was reached by the late Holocene before falling to current sea level positions.

The sea-level curve developed in this study challenges the interpretations of continual Holocene sea level rise in the Gulf of Mexico (GoM) from basal peat data in the Mississippi delta. The beach ridge data in this study does not exhibit the deep-seated subsidence that occurs in the basal peat data and are therefore a more reliable sea level indicator. However, even after correcting for the deep-seated subsidence component in the Mississippi delta, the difference in sea level elevation between two curves cannot be resolved. Therefore, it is appears that both curves are local in nature, and neither is likely representative of Holocene sea-level change for the broader northern GoM.

In addition to contributing to our understanding of Holocene sea-level change for the eastern GoM, results of this research provide context for sea-level conditions during which the Mississippi delta was constructed and can provide insight into future shoreline response to rising sea levels. Improved understanding of Holocene sea-level rise in the northern GoM requires further sea level curve constructions on progradation sandy shorelines along the Mississippi Delta.

Acknowledgments

I thank Dr. Mike Blum for his guidance and patience, as I took an extended path in completion of this thesis. Without Mike's support, I would have not come to KU, thereby missing the opportunity to work on research that I truly enjoy. I would also like to thank Dr. Georgios Tsoflias, who allowed me to use his Geophysical equipment and software and provided support in processing the raw data. Dr. William Johnson provided context for coastal and dune studies and pointed me towards numerous modern beach-ridge studies.

I am grateful to Dr. Bruce Frederick, who assisted in the acquisition of GPR profiles of the Morgan Peninsula beach-ridge sets. Bruce's work on deep-seated subsidence in the Mississippi delta was important in providing context for my research. Brandon Graham taught me how to use the GPR and RTK GPS equipment that allowed collection of the highest resolution data possible. Also, a great thanks goes to the Bon Secour National Wildlife Refuge and Gulf State Park at Lake Shelby, Alabama, which allowed me to perform research and data collection on their land.

Funding for my research was provided through the Kansas Geological Survey, Ray P. Walters Geology Scholarship, Mike Blum's professorship funds, KU Department of Geology, Geological Society of America Graduate Research Grant, and KU Department of Geography and Atmospheric Science.

Finally, I would like to thank my parents who made it possible to obtain my education in the geosciences. I would also like to thank all my friends who I met at KU, including Ben Campanaro, Dakota Burt, Clay Campbell, and Trevor Osorno, who made my time in Lawrence one of the most enjoyable periods of my life.

Table of Contents

1. Introduction 1
2. Background 4
2.1. Post-Glacial Sea-Level Change and Sea-Level Indicators 4
2.2. Early Research on GoM Relative Sea-Level Change 5
2.3. Recent Studies of Coastal Landforms and Deposits as SLIs 6
2.4. Recent Studies of Basal Peats 9
2.5. The Topset-Foreset Break (TFB) and Sea Level Positions 11
3. Methods 13
3.1. Approach 13
3.2. Previous Studies of Sandy Shorelines using GPR 14
3.3. GPR Acquisition and Processing 14
4. Results 17
4.1. Common Midpoint (CMP) Survey Acquisition and Impact on Data Processing 17
4.2. GPR Profiles and Sea-Level Indicators 18
4.2.1. Lake Shelby 18
4.2.2. Little Point Clear 20
4.2.3. Edith Hammock 21
5. Discussion 23
5.1. Interpretation of GPR Profiles 23
5.1.1. Formation of Ridge and Swale Topography 24
5.1.2. GPR Data Attenuation and Discontinuous Reflectors 25
5.1.3. Distinguishing Between Subaerial and Subaqueous Deposits 26
5.2. Topset-Foreset Breaks as Sea Level Proxies 27
5.2.1. Confirming TFBs as SLIs 27
5.2.2. Differences in TFB Depths 28
5.2.3. GPR Depth Calculation 29
5.3. Middle to Late Holocene Morgan Peninsula Sea Level Positions 30

5.3.1. Comparison to Previous Work on the Morgan Peninsula....31
5.4. Comparing Studies of GoM Holocene Sea-Level Change....34
5.4.1. Comparison with the Continual Submergence Model from Basal Peats...35
5.4.2. Comparison with the Continual Submergence Model from Shorelines and Other Locations....36
6. Conclusions....39
7. References....43
8. Figures....51
9. Tables....70

List of Figures

Figure 1.	Comparison of Gulf of Mexico Sea-Level Curves	51
Figure 2.	Thesis Study Area	52
Figure 3.	Aerial Imagery of Ridge and Swale topography	53
Figure 4.	BarSIM numerical models of shoreline response to three Gulf of Mexico Holocene sea-level rise scenarios	54
Figure 5.	200 MHz GPR image of the Morgan Peninsula modern shoreline	55
Figure 6.	OSL Age Locations for the Edith Hammock, Little Point Clear, and Lake Shelby field areas	56
Figure 7.	DEM of the Morgan Peninsula	57
Figure 8.	CMP Survey from the Edith Hammock Shoreline	58
Figure 9.	The Mobile St. GPR Profile Path	59
Figure 10.	Mobile St. GPR Profile	60
Figure 11.	Lake Shelby Profile Path	61
Figure 12.	Lake Shelby GPR Profile	62
Figure 13.	Surfside Road Profile Path	63
Figure 14.	Surfside Road GPR profile	64
Figure 15.	Comparison of Measured Clinoform Angles	65
Figure 16.	Morgan Peninsula RSL Curve	66
Figure 17.	Comparison of the Beach-ridge and Basal Peat SL curves	67
Figure 18.	LiDAR imagery of the Edith Hammock Beach-Ridge set	68
Figure 19.	Along Strike Profile of Northern GoM Deep-Seated Subsidence Rates	69

List of Tables

Table 1. List of All Gulf of Mexico Holocene Sea-Level Studies 70

1. Introduction

Sea level (SL) is an important boundary condition for Earth surface processes and human activities, and as such SL changes over time vary the elevation at which coastal processes operate. Accordingly, past sea-level change is an important area of study by geoscientists in its own right and has become increasingly important to society as a whole due to its potential to provide insight into coastal response to anthropogenically-induced SL rises of the near future (Miller et al. 2013; Kemp et al. 2014, 2015). SL changes in the stratigraphic record are commonly difficult to constrain due to lack of preservation of specific sea-level indicators and to uncertainties in dating. However, Holocene records can be well preserved and chronologically constrained with a variety of dating techniques.

Sea level is measured in different ways (Woodworth 1991, Cazenave et al. 1999, Chen et al. 2005). In this thesis, absolute sea level is the position of the ocean surface relative to the Earth's center of mass at any one time, whereas relative sea level is the position of the sea surface relative to the ocean floor and land surface at a point in time. SL changes over time have both global and local components: over Late Pleistocene and Holocene time scales, global mean sea-level change (ΔGMSL) is used here to refer to changes in the volume of water in the oceans due to growth and decay of glacial ice, whereas relative sea-level change (ΔRSL) refers to the locally-defined changes in the sea surface relative to the land surface (e.g. Peltier and Fairbanks, 2006; Milne et al., 2009). At specific locations, ΔGMSL and ΔRSL can differ significantly due to local to regional uplift or subsidence, or migration of ocean waters around the Earth due to solid-Earth processes (e.g. Peltier, 2004; Lessa and Masselink 2006; Mann et al. 2016).

This thesis addresses Holocene RSL history along the northern Gulf of Mexico (GoM) coast. Numerous previous studies of Holocene ΔRSL have been conducted along the northern GoM shoreline, although a range of views have coalesced in the literature over the last few

decades. One view, derived from the Mississippi Delta region, suggests that radiocarbon-dated basal peats are representative of RSL history for the entire GoM, and reflect continual but decelerating RSL rise (Törnqvist et al. 2004; 2006). Another view contends sandy shoreline systems in non-deltaic parts of the coast indicate that RSL reached present elevations as early as ca. 6000 yrs BP and may have been higher than present at least once since that time (Tanner and Stapor 1972, Morton et al., 2000; Blum et al., 2001, 2002, 2003). The use of basal peats for reconstructing RSL change is widely accepted because of precise dating and clear formative relationships between peats and a contemporaneous sea-level position, but it can be argued that any records of ΔRSL from the Mississippi deltaic depocenter must have a component of subsidence. By contrast, the use of sandy shorelines has been criticized because of limited geochronological controls and a lack of clear relationships between contemporaneous sea level and sea-level indicators within shoreline strata (see Donnelly and Giosan, 2008). Nevertheless, the two contrasting models of Holocene GoM ΔRSL bracket the record of ΔGMSL (Figure 1) (Blum and Roberts, 2012).

This research examines and refines the use of progradational sandy shorelines as sea-level indicators (SLIs) so as to test these alternatives and to develop a more robust history of ΔRSL for the northern GoM shoreline. The study focuses on the Morgan Peninsula, Alabama, located to the east of the Mississippi delta (Figure 2), where long-term subsidence is minimal (Frederick et al., 2018), and where previous research has provided a geomorphological and chronological framework for coastal evolution (Blum et al. 2002; 2003; Otvos and Giardino, 2004; Rodriguez and Meyer, 2006). Ground-penetrating radar (GPR) is used to image stratal geometries in relict sandy shoreline sediments that underlie well-developed beach-ridge plains in this area. Clinoform topset-foreset breaks (TFBs), which represent the boundary between

relatively flat-lying backbeach deposits (the clinoform topset) and the underlying seaward-dipping reflectors of the prograding shoreface (the clinoform foreset), are used here as a proxy for the intertidal zone. Changes through time in the elevation of TFBs are then used to define ΔRSL for this area and evaluate their significance to the broader GoM record of sea-level history.

The results of this study help refine our understanding of Holocene ΔRSL along the northern GoM shoreline. Moreover, results from this study may provide additional longer-term context for modern and near future problems. As previous research has shown, this is an area where significant populations, major ports, and a large proportion of the US hydrocarbon industry are at risk from the effects of future sea-level rise (Thatcher et al. 2010; CPRA 2017).

2. Background

2.1. Post-Glacial Sea-Level Change and Sea-Level Indicators

The record of Holocene Δ RSL is best defined from proxy paleobiological, geochemical, or sedimentological indicators in the stratigraphic record, which are known from modern analogs to form at, or in close proximity to an objective measure of sea level and that can be dated using geochronological techniques. An important concept is the indicative meaning of sea-level indicators (van de Plassche, 1986; Horton 2004), whereby proxy data are tied to a reference water level (e.g. mean SL, mean high tide or high water, mean low tide or low water, etc.), and can define (a) an upper-limiting elevation for sea level at some time in the past (maximum SLIs), (b) a lower-limiting elevation (minimum SLIs), or (c) more precise indicators of high tide, low tide, or intertidal elevations.

On a global scale, sea level was ~120 m below present elevations during the last glacial maximum (LGM), ca. 30-20,000 yrs BP (e.g. Lambeck and Chappell, 2001; Peltier and Fairbanks, 2006; Church et al., 2013; Lambeck et al., 2014). The record of post-LGM (last 20 kyrs) ΔGMSL has been compiled from a wide variety of chronologically-constrained SLIs and locations and begins with SL rise after the LGM at rates of ~10-40 mm/yr, until ca. 7000 yrs BP, when the rate of rise slowed significantly to <1 mm/yr for the remainder of the Holocene (Fairbanks, 1989; Bard et al. 1996; Church et al. 2008). However, beginning in the late 19th century as a result of human-induced climate change, the rate of global SL rise accelerated: mean 20th century GMSL rise from 1.7 mm/yr, accelerating to >3 mm/yr in the last two decades (Beckley et al. 2006; Church and White, 2011; Church et al., 2011; 2013; Ablain et al. 2017; Nerem et al. 2010, 2018).

2.2. Early Research on GoM Relative Sea-Level Change

There is a long history of ΔRSL studies along the northern GoM shoreline. Curray (1961) presented a post-glacial RSL record from the radiocarbon dating of mollusk shells associated with relict shorelines that are now submerged, which were interpreted to show the general trend of SL rise from ca.17,000 to 7000 yrs BP. Frazier (1974) developed a curve for post-glacial ΔRSL based on radiocarbon dates of peats and shells of surf-zone pelecypods and interpreted a stepwise model for SL rise with periods of rapid rise punctuated by intermittent still-stands. Other early studies in eastern Mexico and Mobile Bay used radiocarbon-dated shells in subaerial settings to interpret an oscillating ΔRSL curve, with RSL higher than modern positions at various times during the middle to late Holocene (Behrens 1966, Holmes and Trickey 1974).

Subsequent researchers focused on relict shoreline features, commonly referred to as "beach ridges" (see Taylor and Stone, 1996; Otvos, 2000; Hesp, 2006; Tamura, 2012), which occur at elevations higher than modern SL on GoM barrier islands that are known to be progradational in nature (Bernard et al. 1970; Wilkinson and Basse 1978). Some early authors viewed ridge forms to reflect wave-runup processes (Tanner 1970, Tanner and Stapor 1972, Tanner et al. 1989; 1990) and used the crests of beach ridges as SL indicators. These ridges, varied in height, were known to be late Holocene in age from archaeological data and were therefore hypothesized to record oscillating middle to late Holocene ΔRSL, with one or more highstands that were higher than present (Stapor 1975; Tanner et al. 1989; 1990). The more recent consensus would be the features used by these authors were eolian foredunes, and not specific indicators of sea level, but these early studies defined an alternative view of ΔRSL that exist to this day.

2.3. Recent Studies of Coastal Landforms and Deposits as SLIs

Much of the present discussion was reinvigorated, Blum and Carter (2002), by Morton et al. (2000), and Blum et al. (2001) who identified a series of bay shoreline features along the central Texas coast that were higher than analogous features forming today. Blum and Carter (2002) in a study of beach-ridge features of the Blackjack Peninsula of the central Texas coast identified facies successions typical of progradational wave-dominated shorelines at elevations of 1 m or more above present sea level. Blum and Carter's efforts to use optically-stimulated luminescence (OSL) dating techniques were unsuccessful due to problems with partial bleaching of the sands prior to deposition, hence ages remained poorly known. More broadly, Morton et al. (2000) identified a wide range of coastal landforms and deposits that were partly constrained by ^{14}C ages on shells and that were difficult to explain without sea level having been higher than present in the middle to late Holocene. Blum et al. (2001) examined a specific set of shore-parallel ridges in Copano Bay, southcentral Texas, which produced ^{14}C ages on subtidal foraminifera of ca. 4000-6500 yrs ago, at elevations up to 2 m above present sea level, and concluded that sea level must have been that high or higher at that time. Most recently, Simms et al. (2013) studied the Ingleside shoreline across the San Antonio bay from the Blackjack Peninsula and produced an OSL age of ca. 1,320 yrs ago, at approximately 2 m above MSL.

Regressive, progradational sandy shorelines are widespread along the microtidal GoM shoreline from northern Mexico to Florida (Morton, 1994; Morton et al. 2000). As noted above, shoreline systems of this kind along the northwest Florida coast were the topic of interest for early studies because of the ridge and swale topography that parallels the shoreline and comprises what have been referred to as beach-ridge plains (Stapor 1982) (Figure 3). It is now recognized that the ridge and swale topography indicates the shoreline is overall regressive and has prograded over Holocene time scales, but the ridges themselves are eolian foredunes that

form from deflation of back-beach sediments (Taylor and Stone 1996, Otvos 2001; Blum et al., 2002; see also Tamura, 2012). As a result, ridge heights are unrelated to wave-generated sediment transport and SL, but swales can approximate the former back-beach elevation if there is minimal eolian accumulation, and were therefore argued to approximate maximum SLIs (Blum and Carter, 2002; Blum et al., 2002; 2003).

Regressive sandy shoreline systems have been examined more recently along the Morgan Peninsula and Gulf Shores area in Alabama by Blum et al. (2002; 2003) and Rodriguez and Meyer (2006). Shoreline deposits were initially dated using OSL techniques (Blum et al. 2003), which suggested the deposits formed from ca. 6700-4500 yrs ago, then again during the period ca. 3700-2400 yrs ago. Older middle Holocene ridge and swale topography has swales that occur at elevations of ~0.5 m, similar to modern backbeach environments and that can be flooded at high tide, whereas late Holocene ridge and swale topography has swales 1-2 m above current backbeach elevations (Blum et al. 2003). Blum et al. (2008) combined data from the Texas and Alabama coasts to interpret that RSL reached present positions by at least ca. 6000 yrs ago, and has oscillated within 1-2 m of present since that time (Figure 1).

The Blum et al. (2002; 2003; 2008) results have been criticized from a variety of points-of-view. A parallel study by Rodriguez and Meyer (2006) used GPR imaging and ^{14}C dating to interpret the Alabama sites to record continual RSL rise. Milliken et al. (2008) summarized a variety of data to construct a RSL curve that implies continual submergence, which they argued was representative of the Gulf of Mexico as a whole. The Milliken et al. (2008) study used a variety of ^{14}C dated peats to reconstruct the record prior to ca. 6000 yrs BP but relies on shells recovered from shoreface deposits for the post-6000 yrs BP record. Others argued that beach deposits are not accurate SL indicators because the interface between the eolian cap and

foreshore is difficult to distinguish (Otvos 2001; Rodriguez and Meyer 2006), or that OSL dates were unrealistic, referring to studies on barrier island formation elsewhere (Otvos, 2004). These critiques are in themselves not without problems. First, OSL ages on younger ridge and swale topography in Alabama are consistent with ^{14}C ages collected in similar locations by Rodriguez and Meyer (2006), so ages of these features should not be in dispute. Second, the Rodriguez and Meyer (2006) GPR data shows shoreface clinoform topset-foreset breaks at elevations similar to those forming in the historic period, which is inconsistent with an interpretation of continual submergence at the scale advocated for other parts of the Gulf shoreline. Third, shells used for radiocarbon dating by Milliken et al. (2008) were recovered from cores in shoreface sands that had no independently-defined relationships to SL, and are therefore unconstrained minimum SLIs. Moreover, shells were not recovered from the upper 3 m or so within older middle Holocene beach deposits, although this might indicate these deposits were eolian in origin, or that any shells once present have been removed through leaching processes. Hence, there is no way to constrain how any of the shells used in the Milliken et al. (2008) study correspond to a contemporaneous SL position.

Donnelly and Giosan (2008) took a different approach to criticism of the Blum et al. (2001; 2002; 2003; 2008) interpretations. They noted inconsistencies between the Blum et al, data and interpretations, and data from elsewhere along the Gulf Coast. However, in contrast to the studies of Rodriguez and Meyer (2006) and Milliken et al. (2008), they presented no new data but suggested instead that changes in wave climates as a result in increased storminess would result in constructional wave swells that could build beach deposits at different elevations over time. In this case beach deposits could never be used as reliable SLIs because they change their formative relationship with SL, or their indicative meaning, over time. However, they

provided no evidence to support large variations in wave heights for the Gulf of Mexico during periods of increased storminess, and the Donnely and Giosan (2008) hypothesis would mean that beach deposits of middle Holocene age, which now occur at elevations that are near present SL, would have actually formed when contemporaneous SL positions were 4-5 m below present SL.

Although the multiple highstands model has been criticized, it is not without support from other literature in the GoM. For example, Balsillie and Donoghue (2011) and Donoghue (2011) examined global high-resolution records, noting that multiple sea-level highstands slightly higher than present have been recognized elsewhere, and arguing that data from the Gulf of Mexico shoreline are consistent with those examples.

2.4. Recent Studies of Basal Peats

As noted above, Frazier (1974) used freshwater peats recovered from shallow cores within Holocene deltaic deposits of the Mississippi River to develop a GoM sea-level curve. Peats would have formed at elevations corresponding to mean high tide, i.e. they would correspond to mean high tide if they have not moved vertically since the time of deposition. However, the peats occur within the thick package of Holocene strata and have since subsided an unknown amount due to rapid compaction of underlying deltaic muds (see Törnqvist et al., 2008), hence today they represent minimum paleo-SLIs. By contrast, basal peats, so named because they form in similar freshwater marshes but on non-compacting or subsiding substrates, are viewed as more precise mean high tide paleo-SLIs (Chmura et al., 1987; Törnqvist et al., 2004). Törnqvist et al. (2004; 2006), Gonzalez and Törnqvist (2009) and Yu et al. (2012) have used the depths and ^{14}C age from basal peats (age vs. depth relationship) that formed on compacted Pleistocene deposits to reconstruct RSL change for several locations in the Mississippi delta region. Similar age-depth relationships were defined from different areas within

the delta region (Törnqvist et al., 2006), which were then interpreted to indicate there was no differential subsidence across the area, and that the Pleistocene-Holocene contact was therefore stable and not subsiding.

Because Törnqvist et al. (2004; 2006) considered subsidence or uplift to be negligible, they interpreted the age vs. depth curve for basal peats of the Mississippi delta to define a RSL curve that is representative of the GoM as a whole. The authors also noted that similarities between the Mississippi delta basal-peat record and a ΔRSL curve derived from Caribbean mangrove peats by Toscano and Macintyre (2003) supports this view. Rodriguez et al. (2004), Rodriguez and Meyer (2006) and Milliken et al. (2008) interpreted data from the Texas and Alabama coasts, as discussed above, to be consistent with, and therefore support, the Törnqvist et al. (2004; 2006) model for continual Holocene RSL rise for the GoM (Figure 1) and discounted the Morton et al. (2000) and Blum et al. (2001; 2002; 2003) data from those areas.

A number of authors have raised questions about the assumption that the Pleistocene surface underlying basal peats of the delta region can be regarded as stable and not subsiding (Ivins et al. 2007; Syvitski 2008; Blum et al. 2008; Shen et al. 2017, Kuchar et al., 2018; Frederick et al., 2018). If this is the case, basal peats from the Mississippi Delta region cannot represent precise age vs. depth indicators or regionally significant sea-level indicators (SLI's) unless flexural and other regional-scale deep-seated subsidence processes and rates can be accounted for. Yu et al. (2012) conducted a study of basal peats of the Louisiana Chenier Plain, to the west of thick Holocene deltaic sediment accumulations to test this view. Their data were interpreted to show continual Holocene RSL rise but at a rate that was 0.15 mm ±0.07 mm lower than established by Törnqvist et al. (2004; 2006) for the Holocene delta, whereas studies by Frederick et al. (2019) show these locations reside within the broad region of subsidence

associated with the Mississippi depocenter. Subsequent modeling studies argue that isostatic adjustment is the primary contributor to deep-seated subsidence of the underlying Pleistocene strata (glacial- and sediment-isostatic) with rates of <2 mm/yr (Wolstencroft et al., 2014; Love et al., 2016; Shen et al., 2017). Moreover, recent research has shown that growth faults in the delta region have been active over Holocene time scales and have produced up to 0.7 mm/yr of subsidence (Shen et al., 2017). The interpretations and representative nature of basal-peat data from the delta are therefore perhaps not fully established.

2.5. The Topset-Foreset Break (TFB) and Sea Level Positions

Previous unpublished work used a 2-D numerical model called BarSim by Storms (2003) to simulate the impact of alternative GoM sea-level change scenarios on shoreline trajectory (M. Blum, pers. communication, 2017): this model simulates the topset-foreset break (TFB) and the shoreface clinoform and how they change over time during progradation of the shoreline. Three alternatives were generated using different scenarios for SL change, but with no change through time in wave energy or sediment supply (Figure 4):

- ΔRSL = 0: the TFB maintains the same elevation as the shoreline progrades;
- Steady RSL rise of 5 m: TFBs display a rising trajectory that tracks sea-level change, older shorelines are progressively buried by overwash and lagoonal facies, and older foredune ridges are partially to completely buried and lose their morphological expression;
- RSL rise of 1 m followed by a RSL fall of 1 m, similar to the model of Morton et al. (2000) and Blum et al. (2001; 2003; 2008) for oscillating GoM Holocene sea-level positions: initial and final TFBs occur at similar elevations, but they are separated by

succession of TFBs that are slightly higher, but older shoreline positions and ridge and swale topography are not buried by significant overwash.

M. Blum (pers. communication, 2017) collected a 200 MHz GPR profile of the modern beach on Morgan Peninsula, Alabama, located along the Edith Hammock shoreline in 2008, so as to calibrate modern TFBs to possible SL indicators (Figure 5). These data were processed, corrected for topography, and tied to the modern intertidal zone with survey using an electronic total station. Within the modern backbeach environment, TFBs are clearly recognizable at depths <1 m below the backbeach surface. Topographic survey indicates this contact corresponds to the mean low-tide swash zone and the maximum runup of wave-generated swash bars. TFBs separate two distinctive radar facies (Figure 5): (a) generally flat-lying discontinuous, high-frequency and high-amplitude reflections, which are interpreted to represent backbeach facies deposited by eolian and overwash processes, and (b) discontinuous to mostly continuous, high-frequency, moderate-amplitude reflections that dip seaward at 1-3°, which are interpreted as prograding upper shoreface facies deposited by longshore currents.

This preliminary study demonstrated that TFBs are recognizable in Morgan Peninsula shoreline successions. Following Tamura (2012), relict TFBs *can* be used as paleo-SLIs with two conditions: (1) the elevation of relict TFBs must be referenced to the same benchmark elevation as the modern shoreline, which is the Morgan Peninsula case is the intertidal zone; and (2) seaward-dipping foresets imaged in GPR should have dip angles that are consistent with slopes obtained from measurements of modern foreshores on the peninsula.

3. Methods

3.1. Approach

The two contrasting end-member models of Holocene GoM ΔRSL bracket the record of ΔGMSL (see Figure 1): (1) the continual submergence model places middle to late Holocene sea level at lower positions relative to the global signal, and (2) oscillating but high RSL places sea-level positions at higher positions relative to the global signal. This thesis tests these disparate models at previously dated sandy shoreline systems of the Morgan Peninsula near Gulf Shores, Alabama. The overall approach requires identification of SLIs that are suitable proxies for paleo SL and have a clearly defined indicative meaning. Ground penetrating radar (GPR) and LiDAR are therefore used to identify TFBs in middle and late Holocene shoreline deposits and their elevation relative to present-day mean SL. TFBs are then used as the primary SLI to reconstruct prior SL positions in the study area, assuming they represent the intertidal zone at the time of formation.

The study area is located along the eastern GoM shoreline, to the east of the Mississippi delta (Figure 2) and is considered to be very slowly subsiding to tectonically stable (Blum et al. 2008; Frederick et al. 2019). Previous work shows that Holocene shoreline sediments in the area are widespread and well-developed, and clearly separated from the last Pleistocene interglacial "Pamlico shoreline" by an erosional scarp (Blum et al. 2003). Within the study area, there are three main beach-ridge sets, referred to as Edith Hammock, Lake Shelby, and Little Point Clear (Figure 6). Each set has sufficient chronological control, such that the general time of formation is known: chronological constraints on the Little Point Clear and Lake Shelby beach ridges are provided by OSL ages, which show these features are generally middle Holocene in age (ca. 6600-3800 yrs ago), whereas OSL and radiocarbon ages from the Edith Hammock shoreline

succession place deposition in the late Holocene (ca. 3200-2200 yrs ago) (Blum et al. 2003; Rodriguez and Meyer 2006).

3.2. Previous Studies of Sandy Shorelines using GPR

Many studies have used GPR to image clastic shoreline deposits in the GoM and elsewhere, illustrating that clinoform geometries typical of shoreface progradation can be resolved (Bristow et al., 2000; Bristow and Puchillo, 2006, Jol et al. 1996; Rodriguez and Meyer 2006). More recent studies have shown that the intertidal zone, which is represented by the foreshore to shoreface transition, is identifiable in GPR data, as are downlap surfaces associated with the toesets of seaward-dipping clinoforms (Nielsen 2017; Nielsen and Clemmensen 2009).

Advances in GPR equipment, software, and processing techniques have improved image quality and resolution significantly, which allows for more precise and accurate identification of facies that formed within the intertidal zone. This study builds on the recent work of Nielsen and Clemmensen (2009), and Nielsen (2017), and applies high-resolution GPR imaging to the well-dated sandy shoreline deposits of the Alabama coast.

3.3. GPR Acquisition and Processing

Two-dimensional GPR lines were shot in the Little Point Clear, Lake Shelby, and Edith Hammock areas perpendicular to the orientation of ridge and swale topography (Figure 7) to image TFBs within the underlying progradational sandy shoreline sediments (Jol et al. 1996b; Rodriguez and Meyer 2006). A Sensors and Software pulseEKKO PRO GPR system equipped with a 400V transmitter and 200MHz unshielded antennae was used for data collection. The GPR system was attached to a SMARTCART^{TM} for a rolling single-fold common offset survey with a 0.700 m offset. GPR profiles were collected with a 0.14 m step size and traces were

stacked 32 times to increase the signal-noise ratio. Common midpoint (CMP) surveys for each field area were acquired using 200MHz unshielded antenna to obtain accurate EM wave velocities for data processing and reflector depth calculations.

All GPR data were processed using Sensors and Software EKKO_Project^{TM} software. Processing steps for GPR lines are similar to those of Nielsen and Clemmensen (2009), as described below:

- A DEWOW filter was first applied to the raw data to preserve the desired higher frequency signal and remove lower frequency noise.
- A low-pass frequency filter was then applied to filter frequencies above a percentage of the Nyquist frequency, which filters out high frequency noise.
- A Background Average Subtract filter was applied to remove the average signal and flat lying events that result from antenna interference.
- Gain was applied with a Spreading & Exponential Calibrated Compensation (SEC2) function that preserves more accurately signal amplitude variation resulting from heterogeneities within the subsurface than AGC gain functions.
- Finally, 16 m-long CMP surveys were collected from the Edith Hammock and Lake Shelby beach-ridge plains to determine electro-magnetic (EM) wave velocities of propagation in sediments for time migration and depth calculations.
- GPR data were then time migrated using the velocity of the subsurface media and the 2D Stolt operator to properly image the subsurface (i.e. focus diffracted energy and correct dip angles of reflectors).

Input values for each processing step were adjusted to account for differences in subsurface conditions in each field area.

Elevation data for each GPR line were derived from the 2014 USGS CoNED Topobathymetric DEM of Northern Gulf of Mexico LiDAR data (Figure 8). This digital elevation model (DEM) was created by combining various LiDAR data sets, some of which are not individually available for download. Horizontal accuracy is spatially variable but between 1-3 m, whereas vertical accuracy ranges from 6-23 cm by root mean square (RMS) calculations (USGS 2014). The ArcGIS spatial analyst tool was used to extract topographic profiles and point elevations from GPR profile paths that were recorded from a real-time kinematic (RTK) GPS unit attached to the Smartcart^{TM}. All elevations from the LiDAR DEM are relative to the NAVD88 vertical datum.

In addition to newly acquired GPR data, this study makes use of the legacy dataset shot in 2008: most importantly, the 200 MHz GPR profile of the modern Morgan Peninsula beach, along the Edith Hammock shoreline as described above, was collected to calibrate modern TFBs as a SL indicator (Figure 5). These data were processed using DEWOW and an average gain control function. They were then migrated using a standard velocity corrected for topography, and tied to the modern intertidal zone with precise survey (M. Blum, pers. comm, 2017).

4. Results

Forty 2-D GPR lines were collected in July 2016 from sandy shoreline deposits on the Morgan Peninsula, and proximal to Lake Shelby in Gulf Shores, Alabama (Figure 2). Profiles were taken perpendicular to ridge and swale trends, except for areas that had poor trail clearance or ponded water. For each GPR profile collected, a profile in the opposite direction was also obtained to ensure data reproducibility and accuracy. The results below first discuss GPR data acquisition and processing, including velocity calculations and resolution, then document TFBs in three GPR lines that are representative of the key relationships observed in each study area.

4.1. Common Midpoint (CMP) Survey Acquisition and Impact on Data Processing

16 m CMP surveys were collected from the Edith Hammock and Lake Shelby beach-ridge plain to determine electro-magnetic (EM) wave velocities for time migration and depth calculations (Figure 8): a CMP survey was not possible for from Little Point Clear due to ponding of water, and generally wet conditions. For the Edith Hammock survey, SEC2 gain was applied to CMP data to aid the picking of traces for velocity determination. The first coherent event records the direct air-wave arrival, and has a velocity of 0.30m/ns, whereas the direct ground wave from the dry sand surface layer was recorded at 11.46 ns, with a velocity of 0.133 m/ns that persists until the signal meets the water table at 38.10 ns. Velocities below the water table are 0.060 m/ns, which is consistent with published velocities for saturated sand (Davis and Annan 1989). The Lake Shelby CMP survey confirms EM wave velocities found in Edith Hammock, and, because the Edith Hammock and Lake Shelby surveys yielded similar results, the assumption is made that Little Point Clear would yield the same. Hence EM velocities from the Edith Hammock CMP survey are used in depth calculations and time migration for all three study areas.

Vertical resolution of the GPR data is calculated by the quarter wavelength equation, $\lambda_{1/4} = V/4f$, where λ is the wavelength of the signal, V is the EM wave velocity, and f is the dominant frequency (Yilmaz and Doherty, 1987). Calculations for dry and saturated sand yielded vertical resolutions of 0.21 m and 0.11 m, respectively. These values are used to estimate uncertainty in TFB depths, depending on which layer the TFBs of interest are located, then combined with the resolution of available Lidar data to calculate total vertical error in RSL measurements.

Ground wave and saturated sand velocities were used in depth calculations for each GPR profile: the ground wave velocity was used for the upper 38.10 ns, and velocity through saturated sand was used to calculate depth for the remainder of the profile. Time migration required a two-layer approach because differences in EM wave velocities in dry sand and saturated sand impact reflector geometries during the migration step. After all other processing steps, time migration for both velocities was applied to each profile in EKKO_Project™, creating two images. The images were split by two-way travel time based on the same velocity layering as depth calculations. The separate images were then aligned using the auto-align feature in Adobe Photoshop™ to create a continuous GPR profile.

4.2. GPR Profiles and Sea-Level Indicators

4.2.1. Lake Shelby

Lake Shelby is surrounded by multiple smaller sandy shoreline segments with well-defined ridge-and-swale topography (Blum et al., 2003; Otvos, 2004). Those segments of interest here produced OSL ages that indicate deposition during the middle Holocene and are located within Gulf Shores State Park north of the freshwater Lake Shelby, where they rest against a major scarp that truncates an older Pleistocene shoreline (Figure 9). Ridge and swale

topography associated with the middle Holocene shoreline succession at Lake Shelby is significantly more vegetated than beach ridges at Edith Hammock, and ridge elevations are lower, with maximum heights generally ~1 m above the level of Lake Shelby, which is connected to the Gulf of Mexico and therefore a proxy for sea level (Blum et al. 2003).

GPR data acquisition at Lake Shelby took place on a cleared trail utilized by utility companies, so ridge tops have been flattened and swales have been partially filled along the trail, but disturbance does not penetrate downward to the depths of underlying TFBs. The GPR profile (Figure 10) is 254 m long and was shot north-to-south, crossing three distinct ridges and two intervening swales that were filled with standing water at the time of data collection. Ridges display overall clear reflections from the surface downwards, with clearly recognizable high-amplitude continuous flat-lying reflections that are interpreted to represent eolian and swash zone facies, which in turn overlie seaward-dipping clinoforms that are interpreted to represent upper shoreface. By contrast, reflections from swales tend to be attenuated although underlying seaward dipping clinoforms are generally identifiable. Greater electrical conductivity properties of organic matter and fine-grained sediment within the swales attenuates reflections compared to the ridges. TFBs at the location where OSL ages indicate deposition at ca. 5500 yrs ago are located above the water table at 2.233 m below the land surface (-0.562 m MSL), whereas TFBs at the location where OSL ages indicate deposition at ca. 4640 yrs ago are located above the water table, and 2.003 m below the surface (-0.743 m MSL).

4.2.2. Little Point Clear

Little Point Clear sandy shoreline deposits are of middle Holocene age from OSL ages (Blum et al., 2003) and located in the heavily wooded northwest portion of Morgan Peninsula, within Bon Secour National Wildlife Refuge (Figure 11). The Little Point Clear shorelines include well-defined ridge-and-swale topography and are cross-cut and truncated by the younger Edith Hammock shoreline succession to the south. Similar to Lake Shelby, this area is topographically lower than Edith Hammock and prone to standing water.

GPR data were collected along a poorly-maintained and rutted sand road, in the eastern part of Little Point Clear, where ridges from the west converge: because of standing water, there were sections in the profile where the GPR system had to be transported from its current position along the trajectory of the targeted line and moved to higher and drier ground. However, this location, hereafter referred to as Surfside Road, provides the most detailed and continuous data from Little Point Clear: locations farther west contained more standing water, whereas locations farther east provided less coverage because ridges disappear, are truncated, or merge. The Surfside Road profile includes 508 m of data: the first 80 m were collected on the Edith Hammock shoreline, which can be distinguished in the field from the Little Point Clear shoreline succession by a distinct, mappable scarp, which are interpreted to represent a wave erosion surface, and the remainder came from the Little Point Clear shoreline. The GPR signal was limited by salt-water attenuation after 420 m of data collection, after which there where only shallow weak and flat-lying reflections.

In the Surfside Road GPR profile (Figure 12) The Little Point Clear beach-ridge plain occurs at ~80 m, has a surface relief of ~ 1 m. Attenuation of GPR signal in the Surfside Road profile is the most severe out of all profiles obtained from this study, and is primarily concentrated within the swales. TFBs from the beach-ridge trend that produced an OSL age of

ca. 5520 yrs ago (Blum et al., 2003) are located 2.233 m below the surface (-0.562 m MSL), whereas TFBs from the ridge trend that produced an OSL age of ca. 6620 yrs ago, occur 2.177 m below the surface (-0.917 m MSL).

4.2.3. Edith Hammock

Edith Hammock beach-ridge plains are mostly late Holocene in age (ca. 3310-2400 yrs ago and younger) based on both OSL and ^{14}C ages (Blum et al., 2003; Meyer and Rodriguez, 2006). An older and lower elevation section, the northern end of the survey area most likely correlates to middle Holocene beach-ridge plains of Little Point Clear and Lake Shelby, which in turn abuts a beach-ridge plain of last interglacial age (Blum et al., 2003). Several GPR profiles were collected within the Bon Secour National Wildlife Refuge, however, the GPR profile collected on Mobile Street provides the most continuous data. This profile was collected from south-to-north in the late Holocene portion of the Edith Hammock shoreline succession, beginning at the modern foredune and continuing for 543 m (Figure 13).

As shown in the aerial photo of Figure 13, and evident in the field as well, ridge and swale topography is clearly identifiable, with ridges dominated by unvegetated white sandy areas with interspersed pine trees, and the topographically lower and poorly-drained swales commonly vegetated and filled with standing fresh water. GPR data acquisition was obtained adjacent to the road to avoid the impact of concrete on velocity. However, the effects of road clearing and grading for road construction are evident here as well, as the topography of eolian ridges adjacent to the profile path in the refuge is significantly more pronounced.

Figure 14 displays a 317 m section of the Mobile Street GPR profile, which passes through locations where samples for OSL dating were collected and published by Blum et al. (2003), as well as locations where shell samples for ^{14}C dating were collected and published by

Rodriguez and Meyer (2006). TFBs from the ridge with an OSL age of ca. 2400 yrs ago, occur at 2.824 m below the ground surface (+0.206 m MSL), whereas TFBs from the ridge trend with an OSL age of ca. 3200 yrs ago, occur at 2.795 m below the surface (+0.051 m MSL). Overlying high-amplitude and relatively continuous flat-lying reflections are interpreted to represent eolian and backshore overwash facies, whereas below the TFB, clinoform foresets dip seaward, to the south, at an average of 2.64°, and are interpreted to represent the prograding upper shoreface.

5. Discussion

Clinoform topset-foreset breaks identified in GPR profiles of sandy shoreline successions allow for the determination of middle to late Holocene sea-level positions for the Morgan Peninsula, Alabama and testing alternative views of northern Gulf of Mexico sea-level change. The discussion below will focus on insights from interpretation of GPR profiles as they pertain to RSL for the Morgan Peninsula, as well as comparison of Morgan Peninsula RSL history with records from the Mississippi Delta and Louisiana Chenier Plain. Following this comparison, other previously studied shoreline features are examined for their suitability for study using GPR methods to widen our understanding of Holocene DRSL history for the northern Gulf of Mexico.

5.1. Interpretation of GPR Profiles

Three issues are fundamental to address prior to understanding the nature and significance of GPR data from Morgan Peninsula shoreline successions as sea-level indicators. First, previous workers have used the heights of ridge and swale topography as sea-level indicators. Second, GPR data are collected from ridge and swale topography, which introduces significant variability in shallow subsurface material properties. Third, previous work suggests it can be difficult to differentiate eolian and overwash facies from prograding shoreface deposits using trenches or cores, and therefore define a specific SLI in sandy shoreline deposits.

5.1.1. Formation of Ridge and Swale Topography

Landforms examined in this study are commonly referred to as beach-ridge plains, which are progradational sandy shorelines with characteristic ridge-and-swale topography (Taylor and Stone, 1996). Earlier workers along the northern GoM shoreline treated ridge and swale topography as a product of deposition during wave run-up (Tanner and Stapor 1972, Tanner et al., 1989; 1990). However, ridges are generally eolian features, classically referred to as foredunes, shore-parallel dune ridges that form on the backbeach by eolian sand deposition in the presence of vegetation (Hesp, 2002; 2006). A succession of eolian foredune ridges are then constructed as the shoreline progrades, such that the succession of foredune ridges is actually a signature of a progradational shoreline. However, their morphological expression is only a very crude maximum SLI (e.g. Blum et al., 2002).

Intervening topographic lows, the swales, represent former backbeach environments that have been incorporated into the succession of foredune ridges as the shoreline progrades. Swales may have elevations that are similar to the backbeach when it initially formed, but also can be covered by a variable thickness of eolian and slopewash facies from the foredune environments (Carter 1986; Otvos 2000; Rodriguez and Meyer 2006). Swale elevations are maximum SLIs as well and more closely approximate a former sea-level position than the ridges (e.g. Blum et al., 2002), but there is no specific relationship with an objective measure of sea level due to the variable thickness of eolian and slope wash facies.

5.1.2. GPR Data Attenuation and Discontinuous Reflectors

In the present study, TFBs and seaward-dipping clinoforms observed in GPR images typically lie ~2 m or more below swale surfaces, and TFBs are overlain by a radar facies that are generally dominated by flat-lying parallel reflectors similar to the modern backbeach and, as such are therefore interpreted to represent eolian and swash zone processes responsible for backbeach deposition (Figures 10, 12, 14). However, as the shoreline progrades, and backbeach surfaces are left stranded between successive foredune ridges, they can hold standing water and accumulate organic material and sediment from eolian and slopewash processes as well (Hesp 2002, Tamura 2012). Attenuation of GPR signal within swales attributed to organic matters is recognized as an impediment in the study area: this attenuation impacts reflectors throughout the entire section in the profile, which corresponds to washed out and flat lying events. In this study, attenuation is most severe in the Little Point Clear study area (Figure 12), where the overall landscape is lower in elevation, close to the water table, and susceptible to flooding during extreme high tides and storm surges. Although similarly low in elevation, attenuation was less of a problem at Lake Shelby, and, because the ridge and swale topography of the Edith Hammock shoreline succession is higher in elevation, and swales generally have standing water only after periods of rain, attenuation of the GPR signal was not an issue.

During GPR acquisition, discontinuous facies are also observed in certain ridges and swales throughout the three profiles. An example of this phenomenon can be seen in the Lake Shelby GPR Profile (Figure 10) starting at 160 m and continuing to 205 m. In this section initial EM wave energy in the upper part of the profile returns strong flat-lying reflectors. As the EM wave continues through the underlying media, underlying reflections appear discontinuous and chaotic. Below the chaotic reflectors at ~50 ns seaward-dipping clinoforms appear and continue on through the profile. This appearance of chaotic reflectors in ridges and swales is likely

caused by reorganization of backbeach sediments during high intensity storms. However, to confirm this interpretation, further ground truthing is necessary.

5.1.3. Distinguishing Between Subaerial and Subaqueous Deposits

One major criticism of using beach deposits as SLIs is that shoreface sediment, deposited below sea level, cannot be easily distinguished from overlying eolian foredune or swash and overwash deposits of the backbeach environment in core, which can lead to misinterpreted facies and inconsistent OSL age dates, and misidentification of actual SLIs that have a specific relationship with sea level (Otvos 2001, 2004). Indeed, it can be difficult to determine the depth of the foreshore-shoreface contact within core, hence this issue was avoided in this study.

The GPR approach used here circumvents this issue. Previous workers show that eolian and swash/overwash deposits that represent the clinoform topset can be differentiated from upper shoreface clinoform foresets using GPR data (Jol et al. 1996; Nielsen and Clemmensen 2009), and the TFB, which represents the foreshore to shoreface contact, can be clearly imaged with GPR as well. Moreover, the GPR image of the modern Morgan Peninsula shoreline illustrates how seaward-dipping clinoform foresets underlie flat-lying reflectors of the backbeach and active eolian foredune topset (Figure 5). The intervening radar facies change defines the TFB and corresponds to the intertidal zone.

GPR images in this study do not display any overlying overwash and/or lagoonal facies in the older middle Holocene shoreline deposits of Little Point Clear and Lake Shelby, which would be expected if continual RSL rise had dominated this area (Figure 4). If overwash or lagoonal facies were present, would contain some muds and organic material, which would have a different EM velocity and necessitate a 3-layer model. Moreover, GPR surveys did not encounter and saltwater conditions, which would contribute to highly conductive media and lead

to high signal attenuation (Davis and Annan 1989), thereby making it difficult to image dipping the seaward-dipping reflectors present in this study.

5.2. Topset-Foreset Breaks as Sea Level Proxies

As noted above, TFBs imaged from the modern beach at Edith Hammock correspond to the intertidal zone (M. Blum pers. communication, 2017), and because this section GoM shoreline is microtidal, with a tidal range of 38.3 cm as measured from the NOAA Dauphin Island (2017) water level station, the intertidal zone more generally approximates mean sea level. Clinoform foresets of the modern beach GPR Profile dip seaward at 2-3° (Figure 5), which is consistent with dip angles measured on the modern shoreface by Douglass (2001). Accordingly, this thesis relies on the use of topset-foreset breaks (TFBs) imaged in GPR data from older shoreline successions as the primary SLI.

5.2.1. Confirming TFBs as SLIs

To support the interpretation of relict TFBs from GPR data, and their use as SLIs, this study points to Tamura (2012) who argued that relict clinoform foresets should dip at the same or similar angle as their modern analog counterparts from the same locality. Ten foreset angles were measured from depth-converted GPR profiles presented here to verify that TFBs interpreted from relict shorelines are consistent with modern values. Dip angles were measured for each study area starting at the TFB and ending at the terminus of the time window available for each of the clinoform foresets. Clinoform foresets for the Little Point Clear, Edith Hammock, and Lake Shelby study areas dip seaward at 2.3-3.1° (Figure 15). These values fall within the range of modern shoreface values from the Morgan Peninsula (Figure 15) and are consistent with clinoform dip angles measured in GPR data by Rodriguez and Meyer (2006), which support the use of relict TFBs and seaward-dipping shoreface clinoforms from GPR data as SLIs.

5.2.2. Differences in TFB Depths

The Lake Shelby and Little Point Clear shoreline successions have thin backbeach and eolian facies overlying TFBs, relative to Edith Hammock. For example, Little Point Clear TFBs occur 2.2-2.0 m below the modern land surface, whereas those from Edith Hammock occur ~2.8 m below the surface: Edith Hammock eolian and backbeach thicknesses are therefore on average 0.6-0.8 m thicker than for Little Point Clear and Lake Shelby. These differences underlie the rationale for viewing swale elevations as imprecise maximum SLIs and focusing instead on TFBs. The Edith Hammock shoreline stands out as a topographic ridge in LiDAR DEM and aerial imaging, and the GPR profile cuts across numerous ridges and swales (Figures 9, 18). Despite the overall higher elevation, beach ridges adjacent to the road are only 0.5-1 m higher than the swales, which is consistent with a reduced thickness of eolian sediments due to road construction. Similar differences occur in the Lake Shelby and Little Point Clear study areas, where cleared paths cut through ridges 0.3-0.7 m away from the path.

Rodriguez and Meyer (2006) suggested that the difference in foreshore depths between Little Point Clear and Edith Hammock was due to foreshore aggradation in response to increased sea level and sediment supplies. If this were the case, Little Point Clear TFBs should display a rising trajectory that reflects continuous sea-level rise (see Figure 12), and older TFBs should be covered by thicker flat-lying radar facies. However, TFBs in the Little Point Clear and Lake Shelby GPR profiles occur at similar elevations and are covered by similar thicknesses throughout their profile lengths, which is indicative of normal progradation as opposed to aggradation. Differences in thickness of sediments that overlie the Little Point Clear and Lake Shelby vs. Edith Hammock TFBs are likely due to beach morphodynamics during berm and dune formation (Carter 1986, Hesp 2002, Otvos 2000, Tamura 2012).

5.2.3. GPR Depth Calculation

Subsurface GPR depth calculations used in this study differ significantly from prior beach-ridge studies that used minimum or average EM wave velocities (Bristow and Puchilow 2006; Rodriguez and Meyer 2006; Nielsen and Clemmensen 2009). Instead of determining wave velocities from diffraction analysis, this study used CMP surveys to understand the effect on EM wave velocity with increasing depth at most GPR profile locations (Figure 8). A dual-layer velocity model for calculating depth was chosen to incorporate the effect of unsaturated sand in eolian ridges, which has a high EM velocity (Davis and Annan 1989) and represents the first layer in the depth calculation. Deposits below the freshwater table that have a significantly lower EM velocity and represent the second layer (Davis and Anan 1989).

Use of an average EM velocity from diffraction analyses, as was done in other studies, produces TFBs with elevations that are ~1-1.5 m higher than depths calculated by the two-layer depth model because they underestimate the effect of the dry upper layer on EM velocity. Conversely, depth calculations from the two-layer velocity model used in this study produce subsurface depths greater than using average EM velocities. Therefore, the depths of TFBs are minimum SLIs, as the model fails to account for change in velocity with increasing water saturation of the capillary fringe.

5.3. Middle to Late Holocene Morgan Peninsula Sea Level Positions

Middle to late Holocene RSL positions for the Morgan Peninsula were created combining the TFB depths from beach ridges in all three field areas, OSL geochronology, and elevations extracted from the 2014 USGS CoNED Topobathymetric DEM of the Northern Gulf of Mexico LiDAR data set. All sea level positions from TFBs are interpreted in terms of their indicative meaning relative to NAV88D vertical datum. To calculate the vertical error in each SLI, the LiDAR vertical error of 0.23 m was combined with the minimum GPR resolution of 0.21 m for a total error of 0.43 m. Error terms for OSL ages, adopted from Blum et al. (2003), were applied to the TFB elevations at each site where OSL ages were obtained, such that each site has a vertical (depth) and horizontal (age) range defined by error estimates.

Morgan Peninsula and Lake Shelby SL positions generated through this method are referenced to modern LiDAR elevations, but represent minimum values because the dual-layer velocity approach deployed in this study overestimates depths in GPR (see 5.2.3). Nonetheless, these values are shown in Figure 16 and summarized below:

- Middle Holocene sea level at Little Point Clear was at -0.90 m at 6620 yrs ago, -0.545 m by ca. 5520 yrs ago). These values indicate that sea level was within 1 m of modern elevations by the middle Holocene but was not necessarily higher than modern values.
- Middle Holocene sea level at Lake Shelby was at-0.55 m at ca. 5530 yrs ago and at -0.74 m at ca. 4640 yrs ago (Figure 16). As is the case for Little Point Clear, these values indicate that sea level was within 1 m of modern elevations by the middle Holocene but was not necessarily higher than modern values.

- Late Holocene sea level at Edith Hammock was at +0.075 m by ca. 3320 yrs ago and at 0.205 m at ca. 2240 yrs ago. These values indicate that sea level was within 1 m of modern elevations during the late Holocene and was perhaps a few 10s of cm higher.
- Lower TFB's and a downward trajectory in seaward-dipping reflectors are observed in Edith Hammock shoreline deposits that are younger than ca. 2240 yrs ago and point to a general but very modest sea-level fall.

5.3.1. Comparison to Previous Work on the Morgan Peninsula

There are no early Holocene records imaged in the present study, but Rodriguez and Meyer (2006, Figure 9A) present heritage boomer seismic data from Mobile Bay that show buried clinoform foresets at depths of ~7.5 to 12.5 m below modern sea level just to the north of Little Point Clear, which were interpreted initially to be an extension of the Little Point Clear shoreline by Kindinger et al. (1994). Rodriguez and Meyer (2006) interpreted the clinoform succession to be truncated by a transgressive surface of erosion, after which they were buried by bay mud. Rodriguez and Meyer (2006, Figure 9B) also present a nearby chirp seismic line that imaged bay-fill sediments just 2-3 km to the east of the boomer profile. A core was collected along this line, and provided materials for a series of early-to-middle Holocene ^{14}C ages down to depths of 14 m below sea level, and 11 m below the water-sediment interface. The buried clinoform foresets in the first seismic line are not present in this second location (Rodriguez and Meyer, 2006). From ^{14}C ages in the core, Rodriguez and Meyer (2006) interpreted the transgressive surface of erosion to have formed ca. 4300 yrs BP in response to continual SL rise, close to the time of transition between the Little Point Clear and Edith Hammock shoreline trends.

Rodriguez and Meyer (2006) interpretations of these data merit discussion. For example, seismic data presented in their Figure 9A are not depth-migrated, and they interpret depth using a constant seismic velocity of 1500 m/s for both the water and sediment column: this velocity is appropriate for the water column but may be an underestimate for the sediment column (Press 1966). Hence, depths and thicknesses within the sediment column are underestimated, and clinoform foreset dip angles are greater than what can be measured from the non-migrated seismic data. Nevertheless, at face value, dip angles for these submerged and buried clinoform foresets are <1°, which, as reported above, is significantly less than shoreface dip angles of 2-3° elsewhere in the region. This may indicate (1) these features are not shoreface clinoforms but perhaps deltaic due to their lower/relatively lower angle, (2) that depths indicated on the seismic lines are unrealistic, or (3) that the east-west orientation of the seismic line produces the low apparent dips for clinoforms, which are otherwise dipping to the south. Moreover, the chirp seismic line in Rodriguez and Meyer (2006, Figure 9B), located ~2 km to the east of the first line, does not show the buried clinoform foresets at all, and a core from this site sampled 12 m of dark-gray clay characteristic of a bay environment. Hence, data from this core provides no actual guidance to interpret the age or origin of the buried clinoform foresets in the first seismic line: they could be much older, and/or they could be of a non-shoreface origin, and therefore completely unrelated to clinoform foresets of Little Point Clear.

Rodriguez and Meyer (2006) interpreted sea-level rise during the middle Holocene and late Holocene to correlate to, and be responsible for, development of the erosional scarp between the Edith Hammock Shoreline and Little Point Clear beach-ridge plains, which is imaged in their Figure 4, as well as in Figure 14 herein. Prior to the erosional truncation of the Little Point Clear beach-ridge plain, this shoreline has been inferred to have extended to the mainland spit and

represent the same shoreline succession present in the Lake Shelby area (see Otvos, 2004). This erosional truncation, combined with their interpreted higher TFB elevations for the Edith Hammock shoreline, was in turn interpreted to point to transgressive erosion of the Little Point Clear beach-ridge plain due to SL rise. However, Edith Hammock TFBs imaged along Mobile Street for this study occur at relatively constant elevations, and clinoforms are therefore mostly progradational, with no significant aggradational component, which suggests simple normal regression of the Edith Hammock shoreline after ca. 3310 yrs. ago.

Rodriguez and Meyer (2006) disputed the Blum et al. (2003) interpretation of a late Holocene highstand for the Morgan Peninsula based on the higher elevation Edith Hammock shoreline ridge and swale topography. They argued that such an interpretation would imply the lower elevation Little Point Clear beach-ridge plain would have been flooded with seawater when the Edith Hammock shoreline was forming. Instead, they suggested the difference between the Edith Hammock and Little Point Clear was the result of increased foreshore aggradation by eolian processes during formation of the Edith Hammock shoreline, and that rather a rising eolian to shoreface contact is indicative of continual sea-level rise. However, their GPR study used a single-layer velocity model for saturated sand (EM wave velocity of 0.06 m/ns), and therefore underestimated the EM wave velocity of the upper mostly unsaturated eolian component above the TFBs. This indicates they underestimated the thickness of eolian and other sediments that overlie the Edith Hammock TFBs, resulting in an overestimation of the SLI elevations.

The late Holocene SL position of 0.20 m for the Edith Hammock shoreline measured in this study is lower than that estimated by Blum et al. (2003) from the elevations of swales, and by Rodriguez and Meyer (2006) based on their single-velocity model, and does not require

flooding of the Little Point Clear beach-ridge plain where ridges attain elevations of 0.8-1.9 m above MSL. Furthermore, the higher resolution 200MHz GPR profiles produced in this study do not support the Rodriguez and Meyer (2006) interpretation of increasing topset aggradation through time in the Little Point Clear and Lake Shelby beach-ridge plains. Instead, GPR data presented in this thesis show dominantly progradational clinoform geometries, with little to no aggradational trajectory for the TFBs in the middle Holocene Little Point Clear and Lake Shelby beach-ridge plains, or the late Holocene Edith Hammock shoreline system. The data presented here are therefore best interpreted to show that middle Holocene SL was at -0.9 m to -0.5 m from ca. 6600 yrs ago to ca. 4640 yrs ago, whereas late Holocene SL was up to 0.2 m higher than modern values until ca. 2200 yrs ago, after which time TFBs show a slight downward trajectory that points to -level fall of <0.5 m, Morgan Peninsula GPR data support a total SL change of <1 m since ca. 6600 yrs ago, which is in contrast to continual submergence models, which suggest 5 m of SL rise during this time frame.

5.4. Comparing Studies of GoM Holocene Sea-Level Change

Middle to late Holocene sea-level positions generated for Morgan Peninsula in this study are just the most recent set of published data and interpretations for the northern GoM. Most published data interpret trends that represent either continual Holocene submergence, or middle to late Holocene SL positions that were close to and perhaps slightly higher than modern positions (Table 1). The discussion below summarizes differences of interpretation, as well as the potential for revisiting sea-level change studies in other northern GoM locations.

5.4.1. Comparison with the Continual Submergence Model from Basal Peats

There are significant differences between interpretations of basal-peat data collected from the Mississippi Delta region, which represents the anchor for continual submergence interpretations, and the Morgan Peninsula data generated in this study (Figure 17). As noted above, the Morgan Peninsula record studied here does not extend to the early Holocene, whereas basal-peat data is available for much of the Holocene, with ~100 data points that have high vertical and temporal resolution spanning the last ca. 8000 yrs BP (Törnqvist 2004, 2006; Gonzalez and Törnqvist, 2009; Yu et al. 2012). GoM SL records from basal-peat data are therefore more precise and more continuous, which provides a longer-term context and a more detailed record.

In the Mississippi delta region, the basal-peat approach eliminates the influence of compaction of Holocene deltaic sediment, which is the most significant contributor to total land-surface subsidence (Törnqvist et al., 2008; Blum and Roberts, 2012), but then assumes the Pleistocene surface on which the onlapping peats formed is stable and not subsiding. However, recent work challenges this assumption. Blum et al. (2008) used numerical modeling to show there must be a high-frequency isostatic component from glacial-period unloading (producing uplift) and Holocene post-glacial deltaic sediment loading (producing subsidence) in the Mississippi depocenter relative to the Morgan Peninsula area. Shen et al. (2017) show that growth fault systems just north of the Törnqvist et al. (2004; 2006) basal-peat study locations have mean Holocene throw rates of 0.7 mm/yr, which indicate the Pleistocene surface on which basal peats accumulate is not vertically stable over Holocene time scales. Kuchar et al. (2018) modelled sediment isostatic adjustment for Mississippi Delta region and demonstrated that this component of deep subsidence is greatest in the center of the delta where most loading takes

place (see Figure 8), with rates of 0.3 mm/yr, then decays to the east and west. Frederick et al. (2019) used a high-density subsurface data set to show the long-term subsidence rates for the Mississippi depocenter are 0.2-0.3 mm/yr, whereas for the Morgan Peninsula the long-term rates are <0.1 mm/yr (Figure 19). Collectively, these studies show that assumptions of stability of the pre-Holocene surface in the delta region are difficult to substantiate.

For the present study, SLIs for Morgan Peninsula beach-ridge plains have been adjusted downwards from the earlier work of Blum et al. (2003) due to a direct reliance on TFBs rather than swale elevations and due to the 2-layer velocity model, which provides a more robust estimate of TFB depths. Nevertheless, Morgan Peninsula data still show that sea-level positions since ca. 6600 yrs ago were within 1 m of present positions, whereas basal-peat data from the Mississippi delta region place sea level at -5 m or more at ca. 6000 yrs BP, with a mean RSL rise rate since that time of ~0.8 mm/yr. A long-term subsidence rate of ~0.8 mm/yr in the delta region would therefore be required to reconcile the two different records, a value that is similar to that provided by growth faults alone, let alone the deep-seated subsidence component, or the high-frequency isostatic contribution.

5.4.2. Comparison with the Continual Submergence Model from Shorelines and Other Locations

Several localities along the GoM coast have progradational sandy shorelines, but their origins have been interpreted within the context of the continual submergence model. The most important locations for comparison with the present study are the beach-ridge plains of Galveston Island and Bolivar Peninsula along the east Texas Coast, which is significantly far away from the Mississippi depocenter to have minimal load-induced subsidence, and the

subsurface New Orleans barrier trend (also called Pine Island trend), along the southern margin of Lake Ponchartrain in New Orleans, which is the eastern margin of the deltaic depocenter.

Texas barrier islands have been subdivided into regressive (progradational) vs. transgressive forms (see Bernard et al. 1970; Morton 1994; Wilkinson 1975), with the former dominated by beach-ridge plains like that of the Alabama coast. Galveston barrier island, located just south of Houston, is regressive over Holocene time scales, and displays different generations of beach-ridge plain growth similar to Morgan Peninsula, with an older set of ridge-and-swale topography that is cross-cut and truncated by a younger set. In contrast to the Alabama situation, the older set at Galveston is topographically higher than the younger set, with elevations of 1-2 m above MSL, and is of middle to late Holocene age based on ^{14}C ages from shell hash from ca. 5800-5600 yrs BP (Ricklis, 1994) and from the surf-zone clam *Donax sp*. from ca. 5400-2100 yrs BP (Rodriguez et al. 2004; Milliken et al. 2008). Rodriguez et al. (2006) and Milliken et al (2008) used the depths of preserved and dated *Donax sp.* shells as minimum sea-level indicators to infer continuous sea-level rise, which they argue is similar to that from the Mississippi delta. Other explanations for this trend are described in section 2.0 of this thesis, but the key point is that no actual sea-level indicators exist that can be specifically tied to an independently-derived measure of formative sea level itself.

GPR studies can potentially address this controversy for Galveston Island as well. Beach ridges on Galveston Island were first examined with GPR by Jol et al. (1996), who presented a GPR line along the Galveston 8 Mile Road that displayed clinoform foresets, but results were presented without significant processing or correction for topography. As a result, there is no objective tie to sea level. Nevertheless, 100 MHz GPR profiles image 1-2° seaward-dipping shoreface clinoform foresets similar to those of the Morgan Peninsula (Figure 18), with TFBs

approximately 2.1-2.5 m below the surface. Without appropriate processing and locational information to relate the line to the locations of ^{14}C ages, interpretations can go no farther. Several attempts were made to reimage these relict shoreline deposits, but recently constructed canals and the storm surge that covered Galveston Island during Hurricane Ike have introduced saltwater into the subsurface, which causes GPR signal attenuation.

The New Orleans (aka Pine Island) barrier extends >35 km northeast from the city of New Orleans, parallel to the Lake Pontchartrain shoreline. Saucier (1963) collected a database of 5000 sediment cores to define the extent of the barrier and showed the sand body is buried by up to 10 m of deltaic sediments, with burial depths decreasing significantly from west to east, a trend in burial depth that is consistent with flexure due to load-induced subsidence. Subsequently, Stapor and Stone (2004) obtained ^{14}C ages from articulated single shells collected from quarries in the New Orleans area and proposed the barrier formed during a period of sea-level fall between 4000 yrs BP and 3800 yrs BP. Accepting these ages at face value, the New Orleans barrier correlates to the younger part of the Little Point Clear shoreline, and the older part of the Edith Hammock shoreline, of the present study, as well as smaller barrier islands of the Mississippi coast that have subaerial expression. GPR imaging of the New Orleans barrier was attempted by M. Blum (pers. communication) but was not useful due to the overlying deltaic sediments, which attenuated the GPR signal. Nevertheless, further analyses of the Saucier (1963) data set, further sediment coring to define sea-level indicators and their elevations for the New Orleans barrier and correlatives of the Mississippi coast, and additional geochronological controls would contribute to the discussion of sea-level change and the flexural component of Mississippi delta subsidence.

6. Conclusions

Numerous studies of Holocene sea-level change have been conducted along the northern Gulf of Mexico shoreline, however, alternative views have coalesced in the literature over the last few decades. One model, derived from the Mississippi Delta region, suggests that radiocarbon-dated basal peats are representative of relative sea-level history for the entire GoM, and reflect continual but decelerating sea-level rise (Törnqvist et al. 2004; 2006). Another view contends that sandy shoreline systems in non-deltaic parts of the coast indicate that sea level reached present elevations as early as ca. 6000 yrs BP and may have been higher than present at least once since that time (Morton et al., 2000; Blum et al. 2001, 2002, 2003).

This thesis tests these alternative views using high-resolution GPR imaging to identify clinoform topset-foreset breaks (TFBs) as sea-level indicators in the Edith Hammock, Lake Shelby, and Little Point Clear beach-ridge sets of the Morgan Peninsula and Gulf Shores area of south Alabama. Sea-level indicators in GPR data are identified in space using high resolution GPS data, constrained vertically using LiDAR DEMs, and constrained in time by preexisting OSL age dates. TFBs from continuous GPR profiles for the Edith Hammock, Lake Shelby, and Little Point Clear beach-ridge sets are then used to reconstruct middle and late Holocene sea-level positions for this part of the Gulf of Mexico shoreline.

Key conclusions include:

- TFBs identified in high resolution GPR imaging of sandy shoreline systems are reliable sea-level indicators as long as the modern shoreline is used for calibration. GPR profiling of the modern beach shows that modern TFBs are indicative of the intertidal zone, which approximates mean sea level for this microtidal part of the Gulf of Mexico shoreline (tidal range of 38 cm). Moreover, clinoform foresets imaged with GPR have dip angles that are consistent with independent measurements of the modern Morgan

Peninsula shoreface (Douglas 2001) and with previous studies in the area as well (Rodriguez and Meyer, 2006). Seaward-dipping clinoform foresets imaged in the Edith Hammock, Lake Shelby, and Little Point Clear beach-ridge sets are consistent with these values and provide support for their use as TFBs to reconstruct past sea-level positions.

- GPR data for the Lake Shelby and Little Point Clear beach-ridge plains show that middle Holocene sea level was at -0.90 m by ca. 6620 yrs ago and remained within 1 m of present elevations through the middle Holocene until ca. 4000 yrs ago. GPR images in this study do not display significant thicknesses of flat-lying deposits that might represent overwash and lagoonal facies in middle Holocene beach-ridge plains of Little Point Clear and Lake Shelby, nor were there observable and significant increases in topset thicknesses through the extent of these profiles, which record up 2000-2500 yrs. Hence, these beach-ridge plains were progradational without significant aggradation over that extended period of time. GPR data from this study therefore do not support middle Holocene sea-level positions that were 4-5 m lower than modern, nor continual submergence during this time period. However, they also do not support higher than modern values during the middle Holocene along this part of the northern Gulf of Mexico coast, but instead indicate that sea level was slightly below modern positions.
- GPR data from the Edith Hammock beach-ridge plains show that late Holocene sea level was at +0.075 m relative to modern by ca. 3320 yrs ago, and at +0.205 m by ca. 2200 yrs ago. These interpretations are inconsistent with Rodriguez and Meyer (2006), in part because that study used a single-later velocity model to estimate depth in their GPR profiles, which is here interpreted to mean they underestimated the sediment thickness and therefore argued that the beach ridges support the continual submergence model.

- Late Holocene sea-level positions in this study, as recorded by processed GPR data, are shifted downward from those in Blum et al. (2003), but GPR data from beach-ridge plains of the Morgan Peninsula and Lake Shelby, Alabama continues to support the view found in some previous shoreline studies (e.g. Behrens, 1966; Holmes and Trickey, 1974; Stapor 1975; Tanner et al., 1989; 1990; Morton et al., 2000; Blum et al., 2001; Blum et al 2002; 2003) whereby sea level was very close to present positions prior to ca. 6000 yrs ago: sandy progradational shorelines formed in association with sea level at this position, and sea level has been within ±1 m of present since that time.

The GPR data collection and processing protocols used in this study were successful in improving the identification and use of SLIs within relict progradational sandy shorelines. The results therefore address previous criticisms that data from beach-ridge plains cannot be used as reliable sea-level indicators because it is difficult to distinguish facies contacts in the subsurface that would be related to older sea-level positions (e.g. Otvos, 2001). Instead, collection and processing of GPR data from progradational sandy shorelines provides an effective tool for sea-level reconstruction. A number of researchers have used GPR data to identify other sea-level proxies (Clemmensen and Nielsen 2009, Clemmensen 2017), although this study shows that clinoform topset-foreset breaks can provide accurate sea-level indicators when combined with appropriate velocity models and high-resolution topographic data from which the depths of topset-foreset breaks can be calculated.

Differences between newly defined middle to late Holocene sea-level positions from the Morgan Peninsula, and sea-level positions from basal peats of the Mississippi delta region cannot be resolved without correcting for the effects of subsidence in the delta region, which includes subsidence from Holocene growth fault movement, isostatic adjustments to changes in load, and

the long-term deep-seated component related to the broader Mississippi depocenter (Frederick et al 2019). Both areas produce middle to late Holocene sea-level positions that are local in nature, and neither is likely representative of Holocene sea-level change for the broader northern GoM. However, it may be possible to define a broader Holocene record of sea-level change, and reasons for spatial variability, by identifying topset-foreset breaks in progradational shoreline features to the east and west of the Mississippi Delta along the northern GoM coast.

Sea-level rise as a result of human-induced climate change is an issue that will impact communities along the GoM coast for the next several decades with increasing severity. Similar studies on progradational sandy shorelines may be able to aid future coastal land loss models by providing data on shoreline dynamics over time in response to sea-level change. Increased understanding of past responses to sea-level change along a variety of coastline types should allow for more accurate models to predict the near future.

7. References

2014, Topobathymetric Model of the Northern Gulf of Mexico, 1888 to 2013 DEM, in Survey, U.S.G.S, ed.: NOAA: Data Access Viewer, National Oceanic and Atmospheric Administration.

2017 Datums for 8735180, Dauphin Island AL: NOAA Tides and Currents, NOAA

2017, Louisiana's Comprehensive Master Plan for a Sustainable Coast, Coastal Protection and Restoration Authority of Louisiana

Ablain, M., Legeais, J. F., Prandi, P., Marcos, M., Fenoglio-Marc, L., Dieng, H. B., Benveniste, J., and Cazenave, A., 2017, Satellite Altimetry-Based Sea Level at Global and Regional Scales, *in* Cazenave, A., Champollion, N., Paul, F., and Benveniste, J., eds., Integrative Study of the Mean Sea Level and Its Components: Cham, Springer International Publishing, p. 9-33.

Balsillie, J. H., and Donoghue, J. F., 2011, Northern Gulf of Mexico sea-level history for the past 20,000 years: Gulf of Mexico Origin, Waters, and Biota: Volume III, Geology, v. 3, p. 53-69.

Beckley, B. D., Lemoine, F. G., Luthcke, S. B., Ray, R. D., and Zelensky, N. P., 2007, A reassessment of global and regional mean sea level trends from TOPEX and Jason-1 altimetry based on revised reference frame and orbits: Geophysical Research Letters, v. 34, no. 14.

Behrens, E. W., 1966, Recent emerged beach in eastern Mexico: Science, v. 152, no. 3722, p. 642-643.

Bernard, H., Major Jr, C., Parrott, B., and LeBlanc, R., 1970, Recent sediments of southeast Texas-a field guide to the Brazos alluvial and deltaic plains and the Galveston barrier island complex, University of Texas at Austin, Bureau of Economic Geology.

Blum, M. D., 2017, Personal Communication.

Blum, M. D., and Carter, A. E., 2002, Middle Holocene evolution of the central Texas coast: Gulf Coast Association of Geological Societies Transactions, v. 50, p. 331-341

Blum, M. D., Misner, T. J., Collins, E. S., Scott, D. B., Morton, R. A., and Aslan, A., 2001, Middle Holocene Sea-Level Rise and Highstand at +2 M, Central Texas Coast: Journal of Sedimentary Research, v. 71, no. 4, p. 581-588.

Blum, M. D., Sivers, A. E., Zayac, T., and Goble, R. J., 2003, Middle Holocene sea-level and evolution of the Gulf of Mexico coast, v. 53, p. 64-77.

Blum, M. D. 2008, Morgan Peninsula Modern Shoreline GPR Profile (unpublished)

Blum, M. D., Tomkin, J. H., Purcell, A., and Lancaster, R. R., 2008, Ups and downs of the Mississippi Delta: Geology, v. 36, no. 9, p. 675-678.

Bristow, C. S., Chroston, P. N., and Bailey, S. D., 2000, The structure and development of foredunes on a locally prograding coast: insights from ground-penetrating radar surveys, Norfolk, UK: Sedimentology, v. 47, no. 5, p. 923-944.

Bristow, C. S., and Pucillo, K., 2006, Quantifying rates of coastal progradation from sediment volume using GPR and OSL: the Holocene fill of Guichen Bay, south-east South Australia: Sedimentology, v. 53, no. 4, p. 769-788.

Carter, R., 1986, The morphodynamics of beach-ridge formation: Magilligan, Northern Ireland: Marine Geology, v. 73, no. 3-4, p. 191-214.

Cazenave, A., Dominh, K., Ponchaut, F., Soudarin, L., Cretaux, J. F., and Le Provost, C., 1999, Sea level changes from Topex-Poseidon altimetry and tide gauges, and vertical crustal motions from DORIS: Geophysical Research Letters, v. 26, no. 14, p. 2077-2080.

Chen, J. L., Wilson, C. R., Tapley, B. D., Famiglietti, J. S., and Rodell, M., 2005, Seasonal global mean sea level change from satellite altimeter, GRACE, and geophysical models: Journal of Geodesy, v. 79, no. 9, p. 532-539.

Chmura, G., Aharon, P., Socki, R., and Abernethy, R., 1987, An inventory of 13 C abundances in coastal wetlands of Louisiana, USA: vegetation and sediments: Oecologia, v. 74, no. 2, p. 264-271.

Church, J. A., Clark, P. U., Cazenave, A., Gregory, J. M., Jevrejeva, S., Levermann, A., Merrifield, M. A., Milne, G. A., Nerem, R. S., and Nunn, P. D., 2013, Sea level change: PM Cambridge University Press.

Church, J. A., White, N. J., Aarup, T., Wilson, W. S., Woodworth, P. L., Domingues, C. M., Hunter, J. R., and Lambeck, K., 2008, Understanding global sea levels: past, present and future: Sustainability Science, v. 3, no. 1, p. 9-22.

Curray, J. R., 1961, Late Quaternary sea level: a discussion: Geological Society of America Bulletin, v. 72, no. 11, p. 1707-1712.

Davis, J. L., and Annan, A., 1989, Ground-Penetrating Radar For High-Resolution Mapping Of Soil And Rock Stratigraphy 1: Geophysical prospecting, v. 37, no. 5, p. 531-551.

Donnelly, J. P., and Giosan, L., 2008, Tempestuous highs and lows in the Gulf of Mexico: Geology, v. 36, no. 9, p. 751-752.

Donoghue, J. F., 2011, Sea level history of the northern Gulf of Mexico coast and sea level rise scenarios for the near future: Climatic change, v. 107, no. 1-2, p. 17.

Douglass, S. L., 2001, State of the beaches of Alabama: 2001, University of South Alabama Civil Engineering Department.

Fairbanks, R. G., 1989, A 17,000-year glacio-eustatic sea level record: influence of glacial melting rates on the Younger Dryas event and deep-ocean circulation: Nature, v. 342, no. 6250, p. 637.

Foxgrover, A., 2009, Quantifying the overwash component of Barrier Island morphodynamics: Onslow Beach, NC [Master of Science: William & Mary University, 164 p.

Frazier, D. E., 1974, Depositional episode: their relationship to the Quaternary stratigraphic framework in the northwestern portion of the Gulf basin: The University of Texas at Austin, Bureau of Economic Geology, Geological Circular, v. 74, no. 1, p. 28.

Gonzalez, J. L., and Törnqvist, T. E., 2009, A new Late Holocene sea-level record from the Mississippi Delta: evidence for a climate/sea level connection?: Quaternary Science Reviews, v. 28, no. 17-18, p. 1737-1749.

Hesp, P., 2002, Foredunes and blowouts: initiation, geomorphology and dynamics: Geomorphology, v. 48, no. 1, p. 245-268.

Hesp, P., 2006, Sand beach ridges: definitions and re-definition: Journal of Coastal Research, p. 72-75.

Holmes, N. H., and Trickey, E. B., 1974, Late Holocene sea-level oscillations in Mobile Bay: American Antiquity, v. 39, no. 1, p. 122-124.

Ivins, E. R., Dokka, R. K., and Blom, R. G., 2007, Post-glacial sediment load and subsidence in coastal Louisiana: Geophysical Research Letters, v. 34, no. 16.

Jol, H. M., Smith, D. G., and Meyers, R. A., 1996, Digital Ground Penetrating Radar (GPR): A new geophysical tool for coastal barrier research (examples from the Atlantic, Gulf and Pacific coasts, USA): Journal of Coastal Research, p. 960-968.

Jol, H. M., Smith, D. G., Meyers, R. A., and Lawton, D. C., Ground penetrating radar: high resolution stratigraphic analysis of coastal and fluvial environments, *in* Proceedings GCSSEPM Foundation 17th Annual Research Conference1996 1996, GCSSEPM, p. 153-163.

Kemp, A. C., Dutton, A., and Raymo, M. E., 2015, Paleo Constraints on Future Sea-Level Rise: Current Climate Change Reports, v. 1, no. 3, p. 205-215.

Kindinger, J. L., Balson, P. S., and Flocks, J. G., 1994, Stratigraphy of the Mississippi–Alabama shelf and the Mobile River incised-valley system, in Dalrymple, R.W., Boyd, R., and Zaitlin, B.A., eds., Incised-Valley Systems: Origin and Sedimentary Sequences: SEPM, Special Publication 51, p. 83

Kuchar, J., Milne, G., Wolstencroft, M., Love, R., Tarasov, L., and Hijma, M., 2018, The Influence of Sediment Isostatic Adjustment on Sea Level Change and Land Motion Along the U.S. Gulf Coast: Journal of Geophysical Research: Solid Earth, v. 123, no. 1, p. 780-796.

Kuecher, G. J., 1994, Geologic Framework and Consolidation Settlement Potential of the Lafourche Delta, Topstratum Valley Fill; Implications for Wetland Loss in Terrebonne and Lafourche Parishes, Louisiana [Doctor of Philosophy: Louisiana State University, 391

Lambeck, K., and Chappell, J., 2001, Sea level change through the last glacial cycle: Science, v. 292, no. 5517, p. 679-686.

Lambeck, K., Rouby, H., Purcell, A., Sun, Y., and Sambridge, M., 2014, Sea level and global ice volumes from the Last Glacial Maximum to the Holocene: Proceedings of the National Academy of Sciences, v. 111, no. 43, p. 15296-15303.

Lessa, G., and Masselink, G., 2006, Evidence of a Mid-Holocene Sea Level Highstand from the Sedimentary Record of a Macrotidal Barrier and Paleoestuary System in Northwestern Australia: Journal of Coastal Research, v. 221, p. 100-112.

Love, R., Milne, G. A., Tarasov, L., Engelhart, S. E., Hijma, M. P., Latychev, K., Horton, B. P., and Törnqvist, T. E., 2016, The contribution of glacial isostatic adjustment to projections of sea-level change along the Atlantic and Gulf coasts of North America: Earth's Future, v. 4, no. 10, p. 440-464.

Mann, T., Rovere, A., Schöne, T., Klicpera, A., Stocchi, P., Lukman, M., and Westphal, H., 2016, The magnitude of a mid-Holocene sea-level highstand in the Strait of Makassar: Geomorphology, v. 257, p. 155-163.

Meckel, T. A., ten Brink, U. S., and Williams, S. J., 2006, Current subsidence rates due to compaction of Holocene sediments in southern Louisiana: Geophysical Research Letters, v. 33, no. 11.

Miller, K. G., Kopp, R. E., Horton, B. P., Browning, J. V., and Kemp, A. C., 2013, A geological perspective on sea-level rise and its impacts along the US mid-Atlantic coast: Earth's Future, v. 1, no. 1, p. 3-18.

Milliken, K. T., Anderson, J. B., and Rodriguez, A. B., 2008, A new composite Holocene sea-level curve for the northern Gulf of Mexico: Geological Society of America Special Papers, v. 443, p. 1-11.

Milne, G. A., Gehrels, W. R., Hughes, C. W., and Tamisiea, M. E., 2009, Identifying the causes of sea-level change: Nature Geoscience, v. 2, no. 7, p. 471-478.

Morton, R. A., 1994, Texas Barriers, *in* Davis, R. A., ed., Geology of Holocene Barrier Island Systems: Berlin, Heidelberg, Springer Berlin Heidelberg, p. 75-114.

Morton, R. A., Paine, J. G., and Blum, M. D., 2000, Responses of Stable Bay-Margin and Barrier-Island Systems to Holocene Sea-Level Highstands, Western Gulf of Mexico: Journal of Sedimentary Research, v. 70, no. 3, p. 478-490.

Nerem, R. S., Beckley, B. D., Fasullo, J. T., Hamlington, B. D., Masters, D., and Mitchum, G. T., 2018, Climate-change–driven accelerated sea-level rise detected in the altimeter era: Proceedings of the National Academy of Sciences, v. 115, no. 9, p. 2022-2025.

Nerem, R. S., Chambers, D. P., Choe, C., and Mitchum, G. T., 2010, Estimating Mean Sea Level Change from the TOPEX and Jason Altimeter Missions: Marine Geodesy, v. 33, no. sup1, p. 435-446.

Nielsen, L., Bendixen, M., Kroon, A., Hede, M. U., Clemmensen, L. B., Webetaling, R., and Elberling, B., 2017, Sea-level proxies in Holocene raised beach ridge deposits (Greenland) revealed by ground-penetrating radar: Sci Rep, v. 7, p. 46460.

Nielsen, L., and Clemmensen, L. B., 2009, Sea-level markers identified in ground-penetrating radar data collected across a modern beach ridge system in a microtidal regime: Terra Nova, v. 21, no. 6, p. 474-479.

Otvos, E. G., 2000, Beach ridges — definitions and significance: Geomorphology, v. 32, no. 1-2, p. 83-108.

Otvos, E. G., 2001, Assumed Holocene Highstands, Gulf of Mexico: Basic Issues of Sedimentary and Landform Criteria: Discussion: Journal of Sedimentary Research, v. 71, no. 4, p. 645-647.

Otvos, E. G., 2004, Holocene Gulf levels: recognition issues and an updated sea-level curve: Journal of Coastal Research, p. 680-699.

Otvos, E. G., and Giardino, M. J., 2004, Interlinked barrier chain and delta lobe development, northern Gulf of Mexico: Sedimentary Geology, v. 169, no. 1, p. 47-73.

Peltier, W. R., 2004, GLOBAL GLACIAL ISOSTASY AND THE SURFACE OF THE ICE-AGE EARTH: The ICE-5G (VM2) Model and GRACE: Annual Review of Earth and Planetary Sciences, v. 32, no. 1, p. 111-149.

Peltier, W. R., and Fairbanks, R. G., 2006, Global glacial ice volume and Last Glacial Maximum duration from an extended Barbados sea level record: Quaternary Science Reviews, v. 25, no. 23, p. 3322-3337.

Plassche, O. v. d., and Van de Plassche, O., 1986, Sea-level research : a manual for the collection and evaluation of data, Norwich, Norwich : Geo Books.

Press, F., 1966, Seismic velocities: Handbook of physical constants, p. 195-218.

Ricklis, R. A., and Baker, B. W., 1994, Aboriginal life and culture on the upper Texas coast: archaeology at the Mitchell Ridge site, 41GV66, Galveston Island, Coastal Archaeological Research, Incorporated.

Rodriguez, A. B., 1999, Sedimentary facies and evolution of Late Pleistocene to recent coastal lithosomes on the east Texas shelf [Doctor of Philosophy: Rice University.

Rodriguez, A. B., Anderson, J. B., and Taviani, M., 1999, Sedimentary facies and genesis of Holocene sand banks on the east Texas inner continental shelf: SPECIAL PUBLICATION-SEPM, v. 64, p. 165-178.

Rodriguez, A. B., and Meyer, C. T., 2006, Sea-Level Variation During the Holocene Deduced from the Morphologic and Stratigraphic Evolution of Morgan Peninsula, Alabama, U.S.A: Journal of Sedimentary Research, v. 76, no. 2, p. 257-269.

Saucier, R. T., 1963, Recent Geomorphic History of the Pontchatrain Basin, Louisiana: Louisiana State University, 114 p.

Shea, P., and Karen, E. R., 1990, Relative Sea-Level Rise in Louisiana and the Gulf of Mexico: 1908-1988: Journal of Coastal Research, v. 6, no. 2, p. 323-342.

Shen, Z., Dawers, N. H., Törnqvist, T. E., Gasparini, N. M., Hijma, M. P., and Mauz, B., 2017, Mechanisms of late Quaternary fault throw-rate variability along the north central Gulf of Mexico coast: implications for coastal subsidence: Basin Research, v. 29, no. 5, p. 557-570.

Simms, A. R., Anderson, J. B., DeWitt, R., Lambeck, K., and Purcell, A., 2013, Quantifying rates of coastal subsidence since the last interglacial and the role of sediment loading: Global and Planetary Change, v. 111, p. 296-308.

Stapor, F. W., and Stone, G. W., 2004, A new depositional model for the buried 4000 yr BP New Orleans barrier: implications for sea-level fluctuations and onshore transport from a nearshore shelf source: Marine Geology, v. 204, no. 1, p. 215-234.

Stapor, F. W., and Tanner, W. F., 1975, Hydrodynamic implications of beach, beach ridge and dune grain size studies: Journal of Sedimentary Research, v. 45, no. 4, p. 926-931.

Stapor Jr, F. W., 1982, Beach ridges and beach ridge coasts, Beaches and Coastal Geology, Springer, p. 160-161.

Storms, J. E. A., Weltje, G. J., van Dijke, J. J., Geel, C. R., and Kroonenberg, S. B., 2002, Process-Response Modeling of Wave-Dominated Coastal Systems: Simulating Evolution and Stratigraphy on Geological Timescales: Journal of Sedimentary Research, v. 72, no. 2, p. 226-239.

Syvitski, J. P. M., 2008, Deltas at risk: Sustainability Science, v. 3, no. 1, p. 23-32.

Tamura, T., 2012, Beach ridges and prograded beach deposits as palaeoenvironment records: Earth-Science Reviews, v. 114, no. 3-4, p. 279-297.

Tanner, W., and Stapor, F., 1972, Precise control of wave run-up in beach ridge construction: Zeitschrift fur Geomorphologie.

Tanner, W. F., 1971, Growth rates of Venezuelan beach ridges: Sedimentary Geology, v. 6, no. 3, p. 215-220.

Tanner, W. F , 1990, Origin of barrier islands on sandy coasts , Gulf Coast Association of Geological Societies Transactions Vol. 40, Pages 819-823.

Tanner, W. F., Demirpolat, S., Stapor, F. W., and Alvarez, L., 1989, The Gulf of Mexico late Holocene sea level curve: Transactions of the Gulf Coast Association of Geological Societies, v. 39, p. 553-562.

Taylor, M., and Gregory, W. S., 1996, Beach-Ridges: A Review: Journal of Coastal Research, v. 12, no. 3, p. 612-621.

Thatcher, C. A., Brock, J. C., and Pendleton, E. A., 2013, Economic Vulnerability to Sea-Level Rise Along the Northern U.S. Gulf Coast: Journal of Coastal Research, v. 63, no. SI, p. 234-243.

Törnqvist, T. E., Bick, S. J., van der Borg, K., and de Jong, A. F. M., 2006, How stable is the Mississippi Delta?: Geology, v. 34, no. 8, p. 697-700.

Törnqvist, T. E., González, J. L., Newsom, L. A., van der Borg, K., de Jong, A. F. M., and Kurnik, C. W., 2004, Deciphering Holocene sea-level history on the US Gulf Coast: A high-resolution record from the Mississippi Delta: Geological Society of America Bulletin, v. 116, no. 7-8, p. 1026-1039.

Toscano, M. A., and Macintyre, I. G., 2003, Corrected western Atlantic sea-level curve for the last 11,000 years based on calibrated 14C dates from Acropora palmata framework and intertidal mangrove peat: Coral Reefs, v. 22, no. 3, p. 257-270.

Wilkinson, B. H., 1975, Matagorda Island, Texas: The Evolution of a Gulf Coast Barrier Complex: Geological Society of America Bulletin, v. 86, no. 7, p. 959-967.

Wilkinson, B. H., and Basse, R. A., 1978, Late Holocene history of the Central Texas coast from Galveston Island to Pass Cavallo: Geological Society of America Bulletin, v. 89, no. 10, p. 1592-1600.

Wolstencroft, M., Shen, Z., Törnqvist, T. E., Milne, G. A., and Kulp, M., 2014, Understanding subsidence in the Mississippi Delta region due to sediment, ice, and ocean loading: Insights from geophysical modeling: Journal of Geophysical Research: Solid Earth, v. 119, no. 4, p. 3838-3856.

Woodworth, P. L., 1991, The Permanent Service for Mean Sea Level and the Global Sea Level Observing System: Journal of Coastal Research, v. 7, no. 3, p. 699-710.

Yilmaz, O., and Doherty, S. M., 1987, Seismic Data Processing (Investigations in Geophysics, Vol 2), Tulsa, Oklahoma, Society of Exploration Geophysicists, Society of Exploration Geophysicists.

Yu, S.-Y., Törnqvist, T. E., and Hu, P., 2012, Quantifying Holocene lithospheric subsidence rates underneath the Mississippi Delta: Earth and Planetary Science Letters, v. 331-332, p. 21-30.

8. Figures

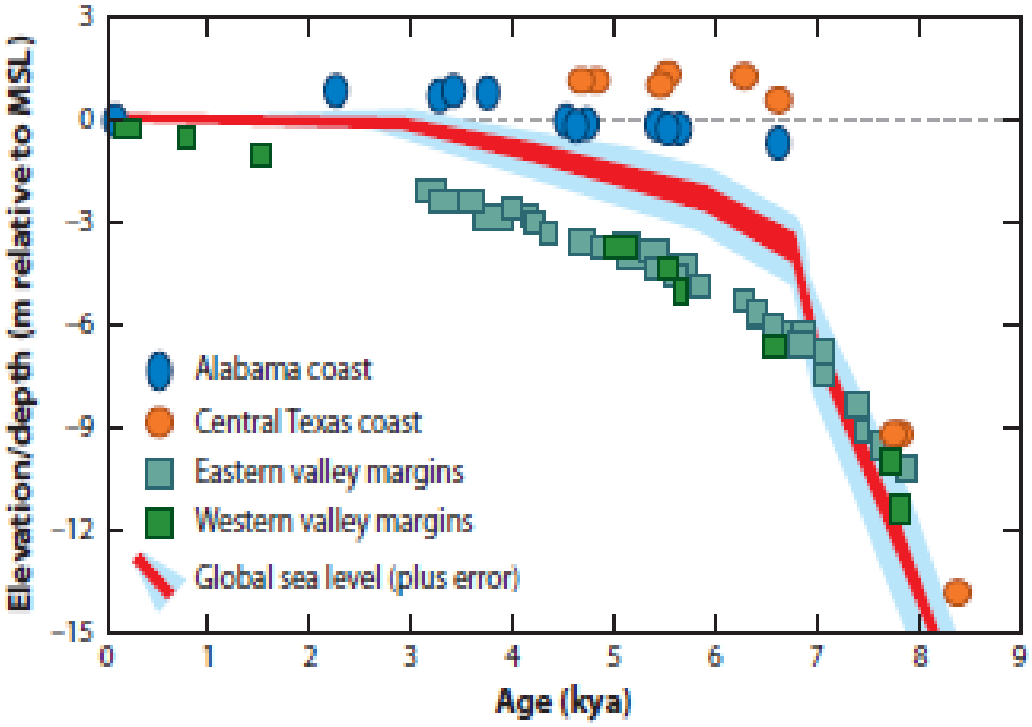

Figure 1. Representation of different sea-level reconstructions for the Gulf of Mexico (based on Tornqvist et al., 2004; 2006; Blum et al., 2001; 2002; 2003), compared to a global sea-level curve (after Church et al., 2008). Reconstructions from the Mississippi delta based on basal-peat data and reconstructions from locations outside the delta region from dating of shoreline deposits correspond closely with the global curve during the early Holocene until ca. 7 ka, then diverge from each other after that. Modified from Blum and Roberts (2012).

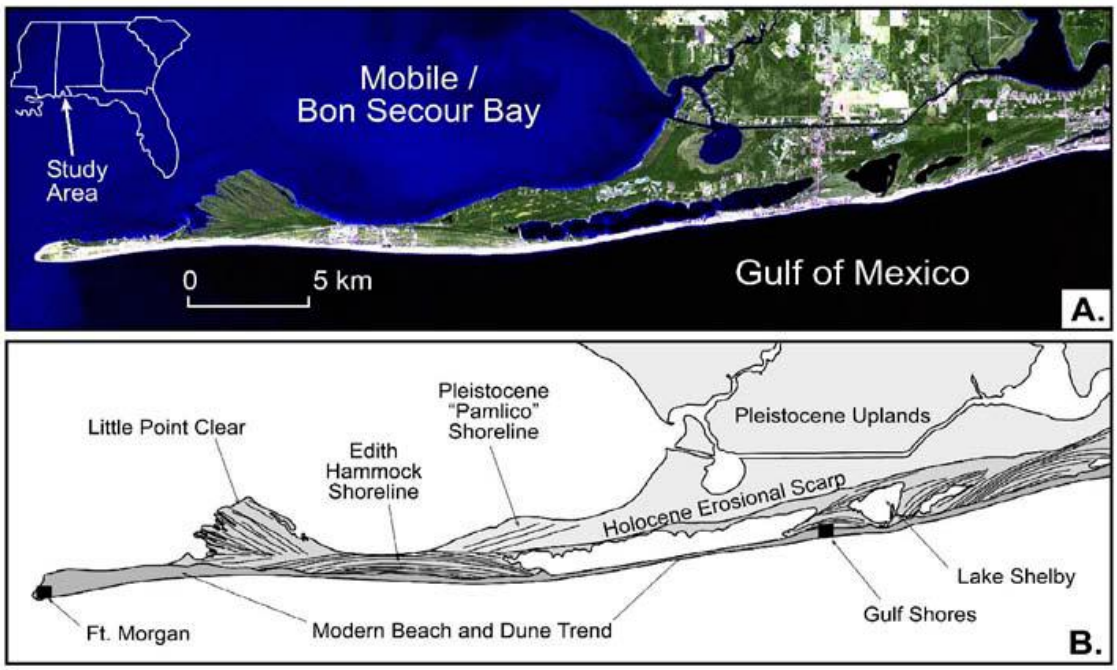

Figure 2. Location of the Morgan Peninsula and Gulf Shores, Alabama field areas along the eastern Gulf of Mexico shoreline. Adapted from Blum et al. (2003).

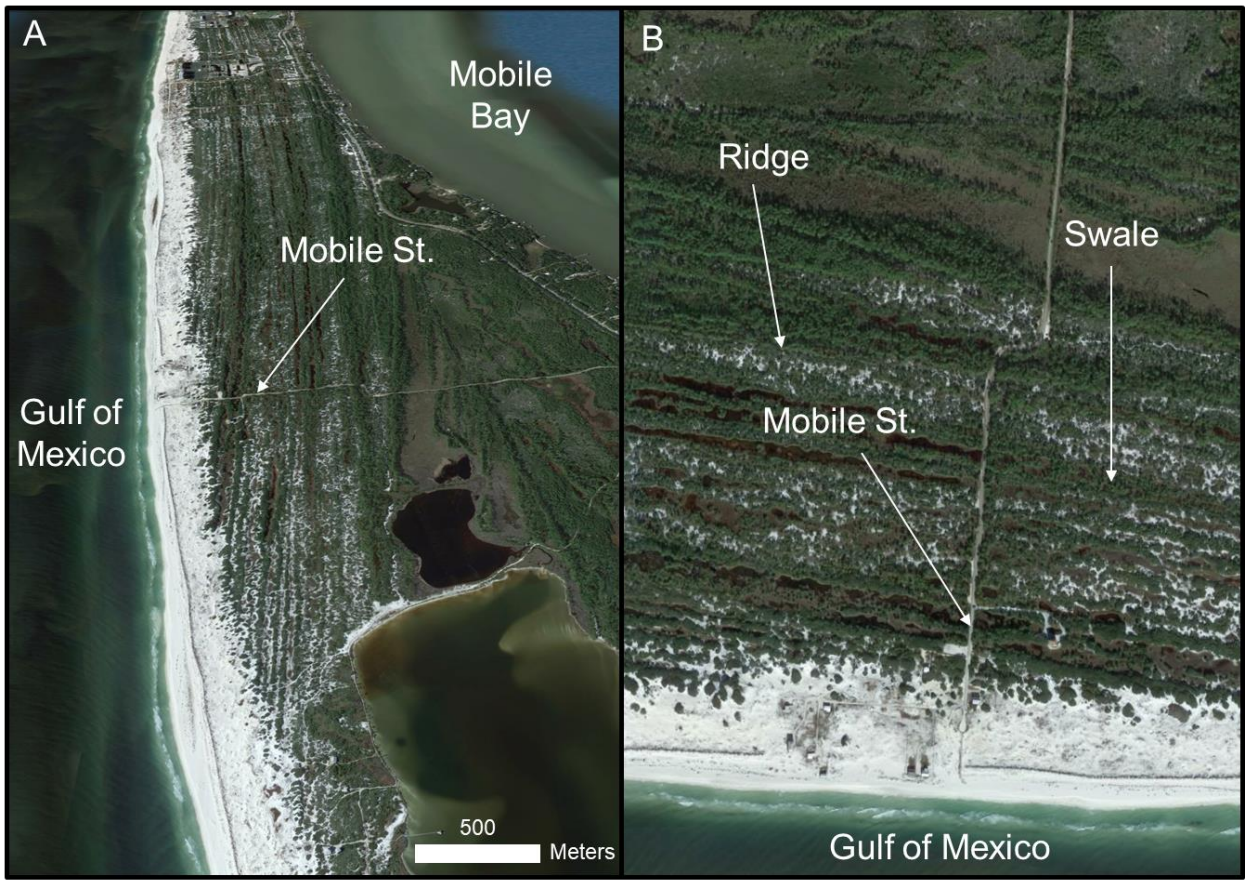

Figure 3. Google Earth (2018) images of beach-ridge plains of the Morgan Peninsula. (A) An oblique along-strike view of the Edith Hammock beach-ridge plains, which extends along the coast for ~12 km. (B) A detailed vertical view of the ridge and swale topography that is indicative of a prograding sandy shorelines: ridges are clearly visible using satellite imagery and aerial photography, but can be subtle and difficult to locate on the surface.

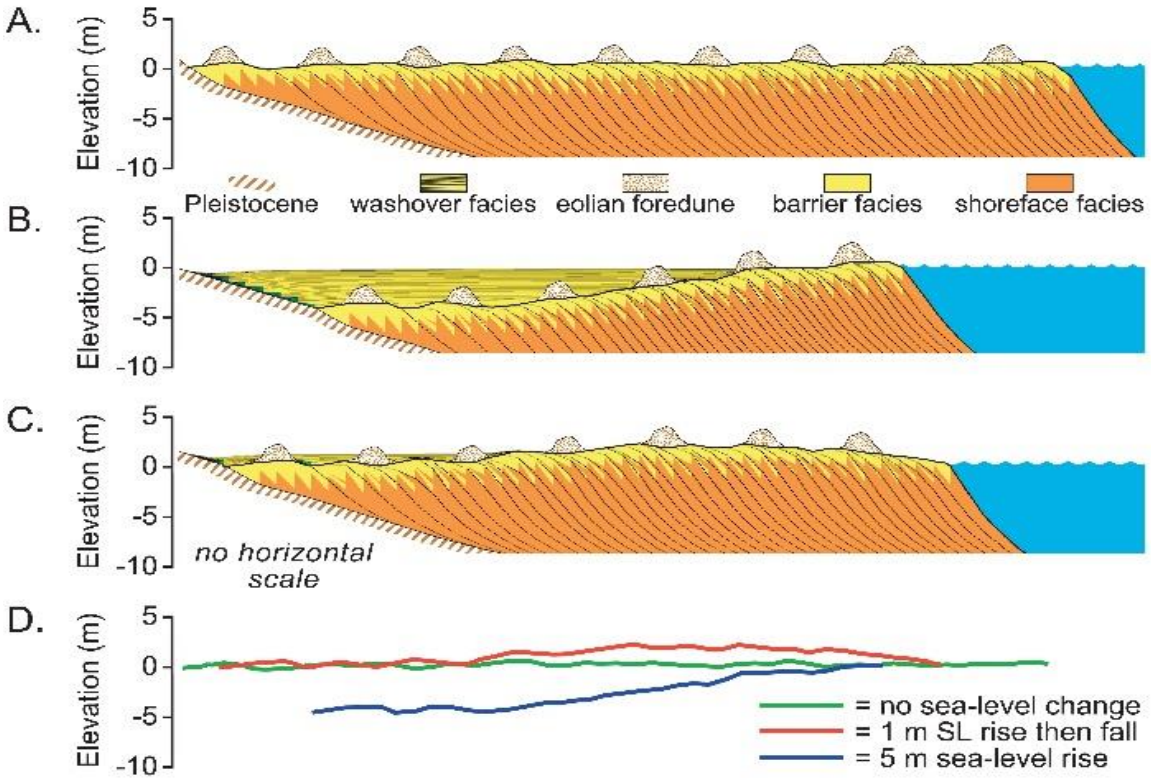

Figure 4. BarSIM Numerical models of shoreline response to three Gulf of Mexico Holocene sea-level rise scenarios using BarSIM (Storms reference) (A) Simulation of topset-foreset breaks with simple progradation and no relative sea-level change, illustrating no change in elevation of topset-foreset breaks. (B) Simulation of topset-foreset breaks with continual RSL rise of 5 m total, illustrating a generally rising trajectory. Note the narrow width of the beach-ridge plain ridge and swale topography and increasing thickness of washover facies with increasing progradation. (C) Simulation of topset-foreset breaks with 1 m of sea-level rise then fall, illustrating a modest rising then falling trajectory. (D) Trace of the topset-foreset break for each simulation (from M. Blum, pers. communication, 2017).

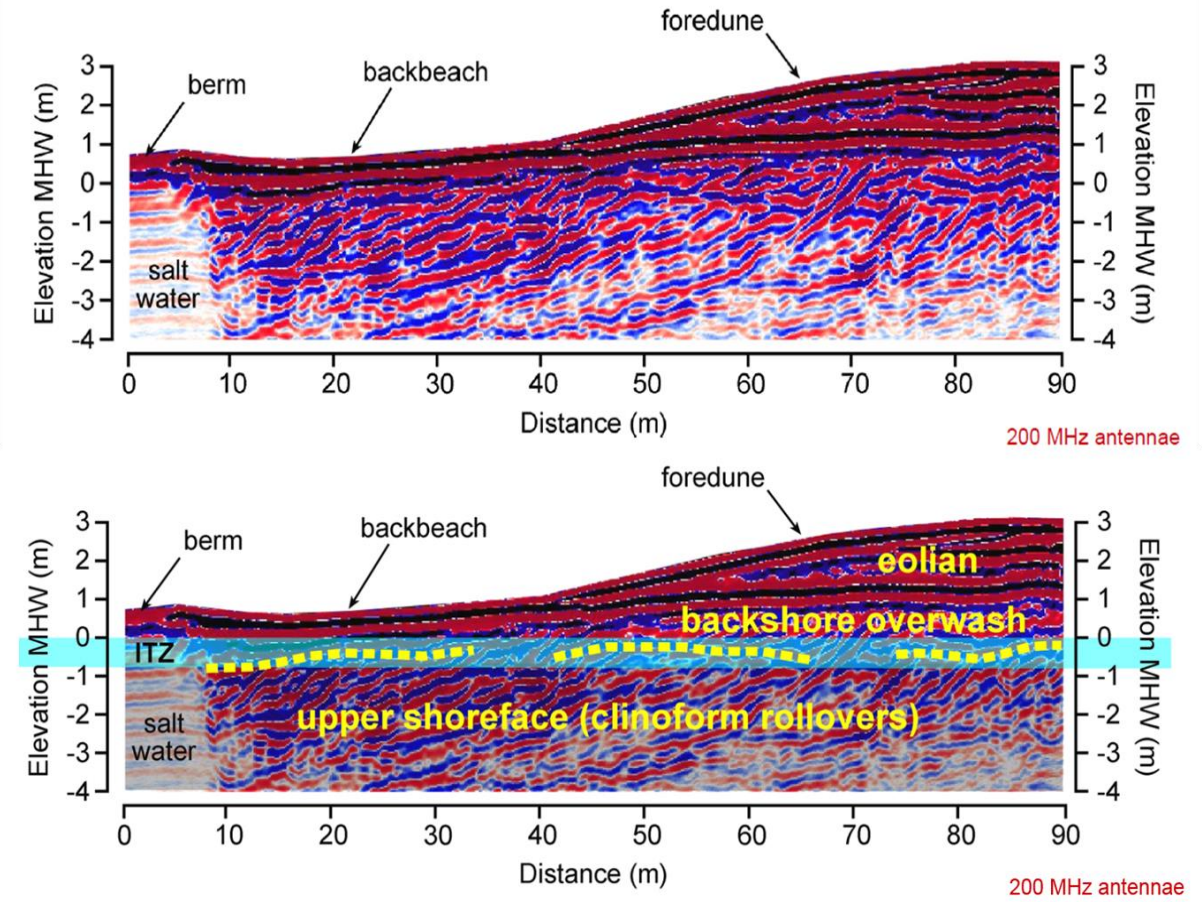

Figure 5. The 200 MHz GPR image from the modern beach on the Morgan Peninsula, which can be used to calibrate topset-foreset breaks as sea-level indicators (Blum 2008). (A) Depth-migrated and topography-corrected but uninterpreted GPR profile. (B) Interpreted profile, showing the position of the intertidal zone (ITZ) relative to topset-foreset breaks (light blue rectangle), which lies between mean high water (MHW) and mean low water (MLW). Topset-foreset breaks represents the transition from the flat lying backshore overwash and eolian facies (the topset) to the seaward-dipping clinoform foresets of the shoreface.

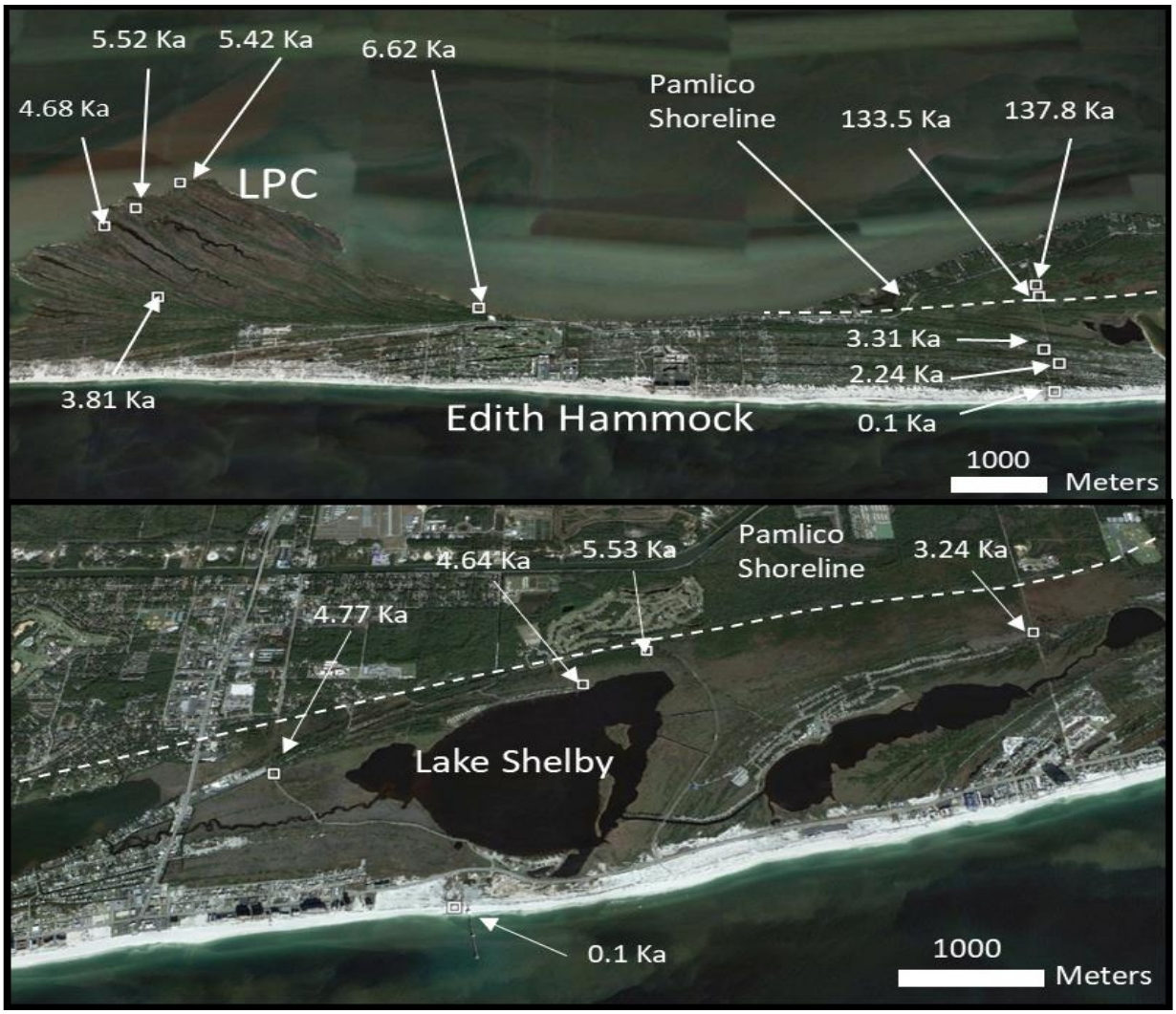

Figure 6. Locations for OSL ages for the Edith Hammock (Late Holocene), Little Point Clear (Middle Holocene) and Lake Shelby (Middle Holocene) beach-ridge plain field areas (modified from Blum et al., 2003).

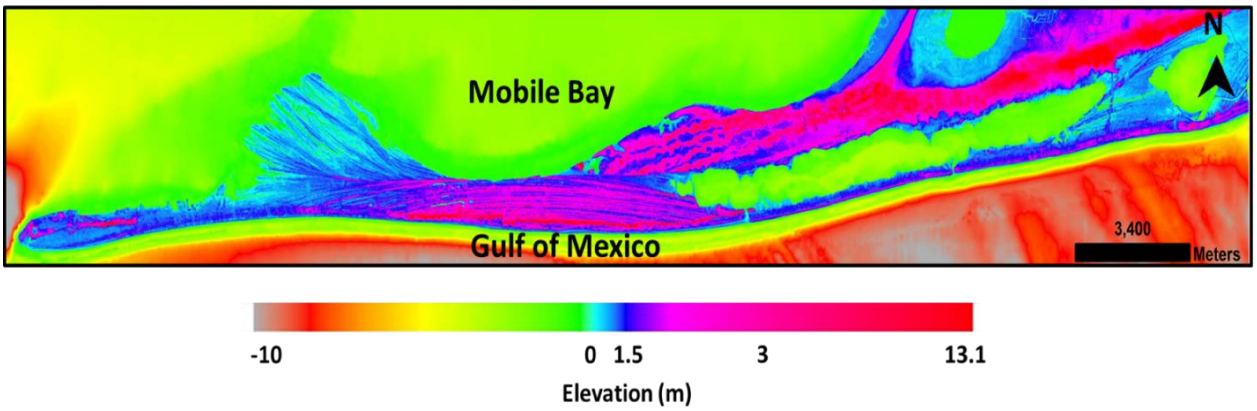

Figure 7. LiDAR digital elevation model (DEM) of the Morgan Peninsula utilized for defining elevations of beach-ridge plains, and topset-foreset breaks imaged in GPR data. Obtained from the 2014 USGS CoNED Topobathymetric DEM of Northern Gulf of Mexico.

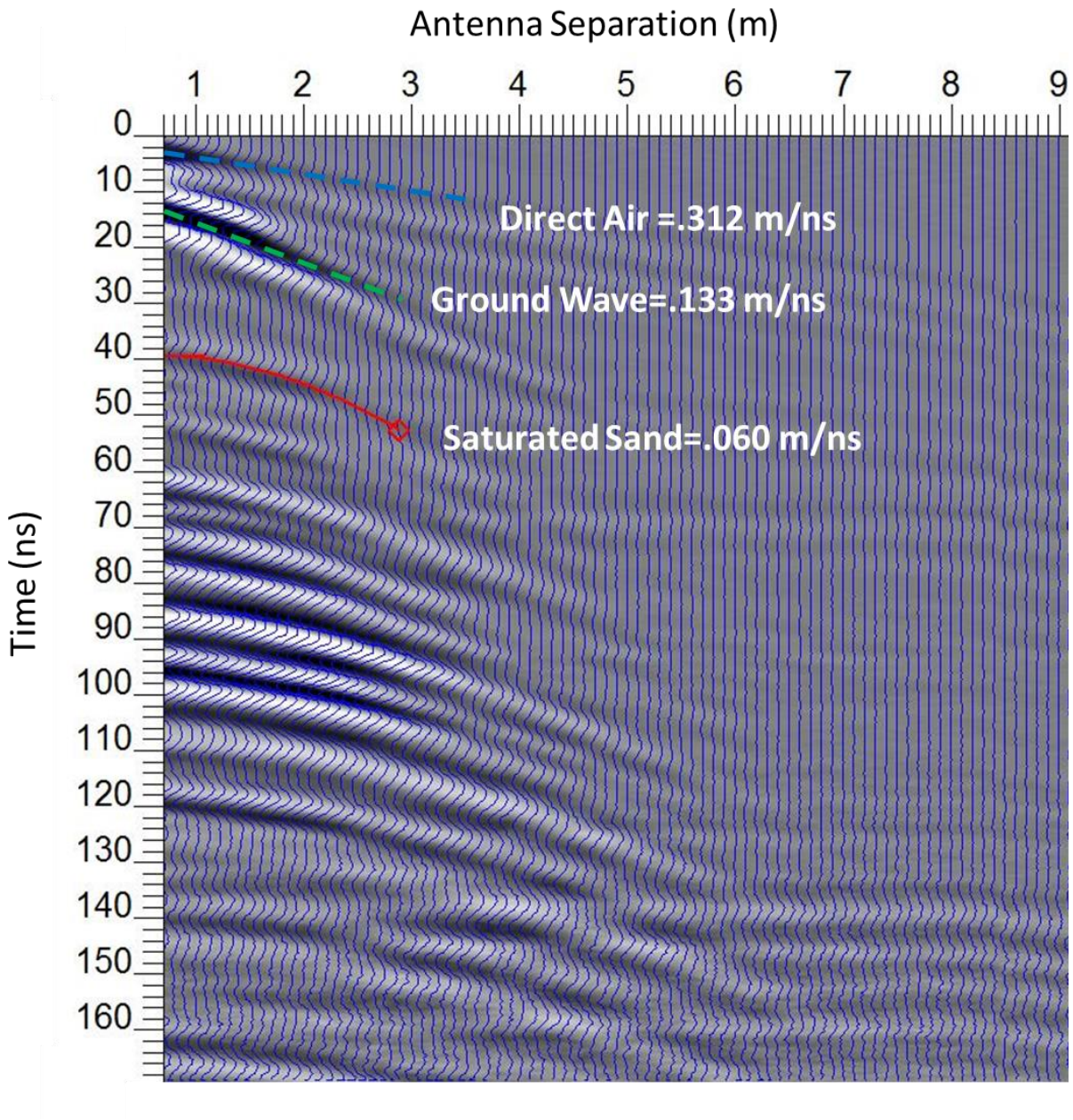

Figure 8. The 9 m section of the original 16 m CMP survey from the Edith Hammock Shoreline used for development of the velocity model. Image includes a standard SEC2 gain, which improves reflection strength and aids in picking traces for velocity determination.

/

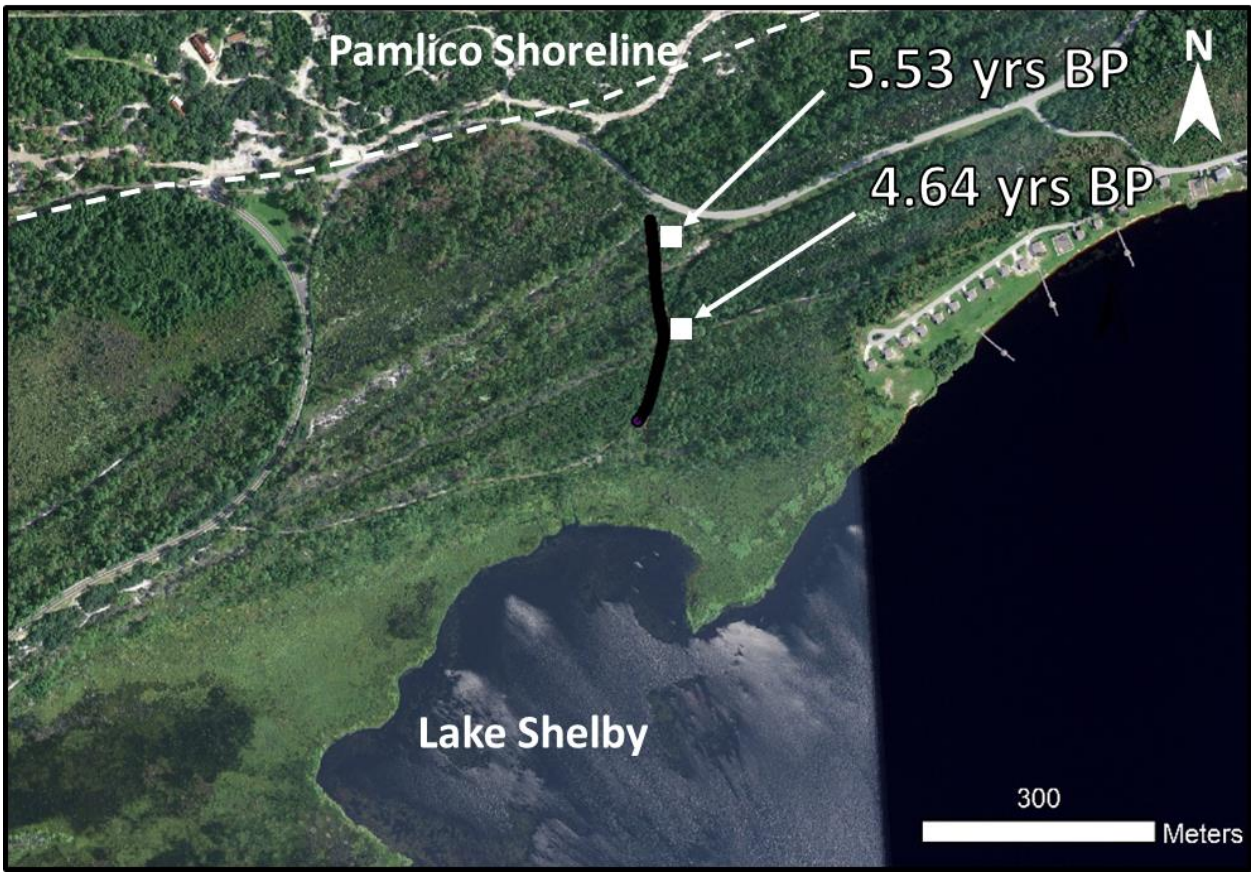

Figure 9. 2014 NAIP aerial image of the Lake Shelby profile path. Imagery obtained from 2014 USDA NAIP dataset

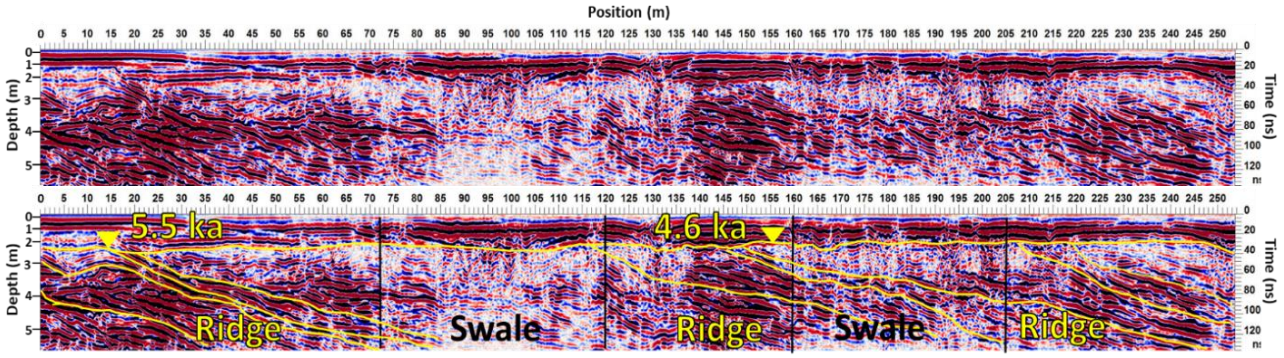

Figure 10. Uninterpreted and interpreted sections of the Lake Shelby GPR profile. The topset-foreset break and the general dips of seaward-dipping shoreface clinoform foresets are highlighted with yellow lines on the bottom image.

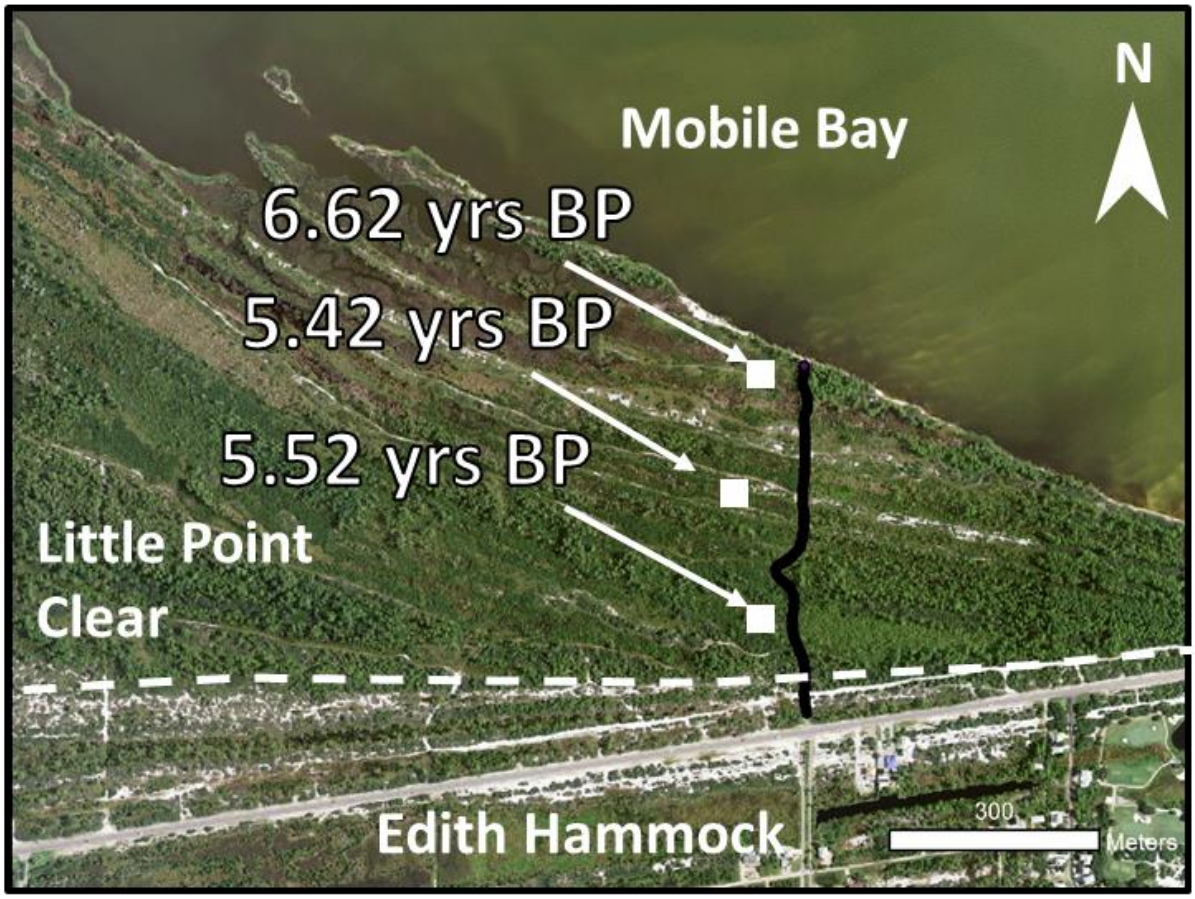

Figure 11: 2014 NAIP imagery of the Surfside Road profile path in the Little Point Clear beach ridge set. This beach ridge set has more swales which tend to pond water, making GPR and CMP acquisition difficult. Imagery obtained from 2014 USDA NAIP dataset

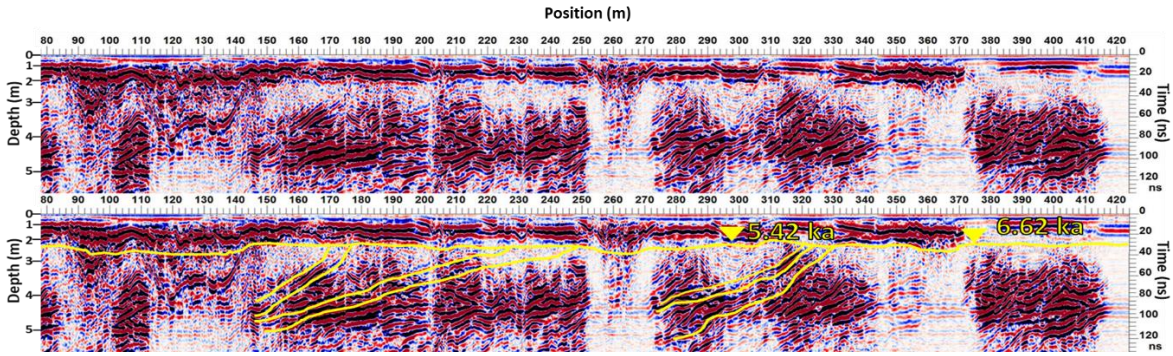

Figure 12. Uninterpreted and interpreted sections of the 420 m Surfside Road GPR profile on the Little Point Clear beach-ridge plain. The topset-foreset break and the general dips of seaward-dipping shoreface clinoform foresets are highlighted with yellow lines on the bottom image.

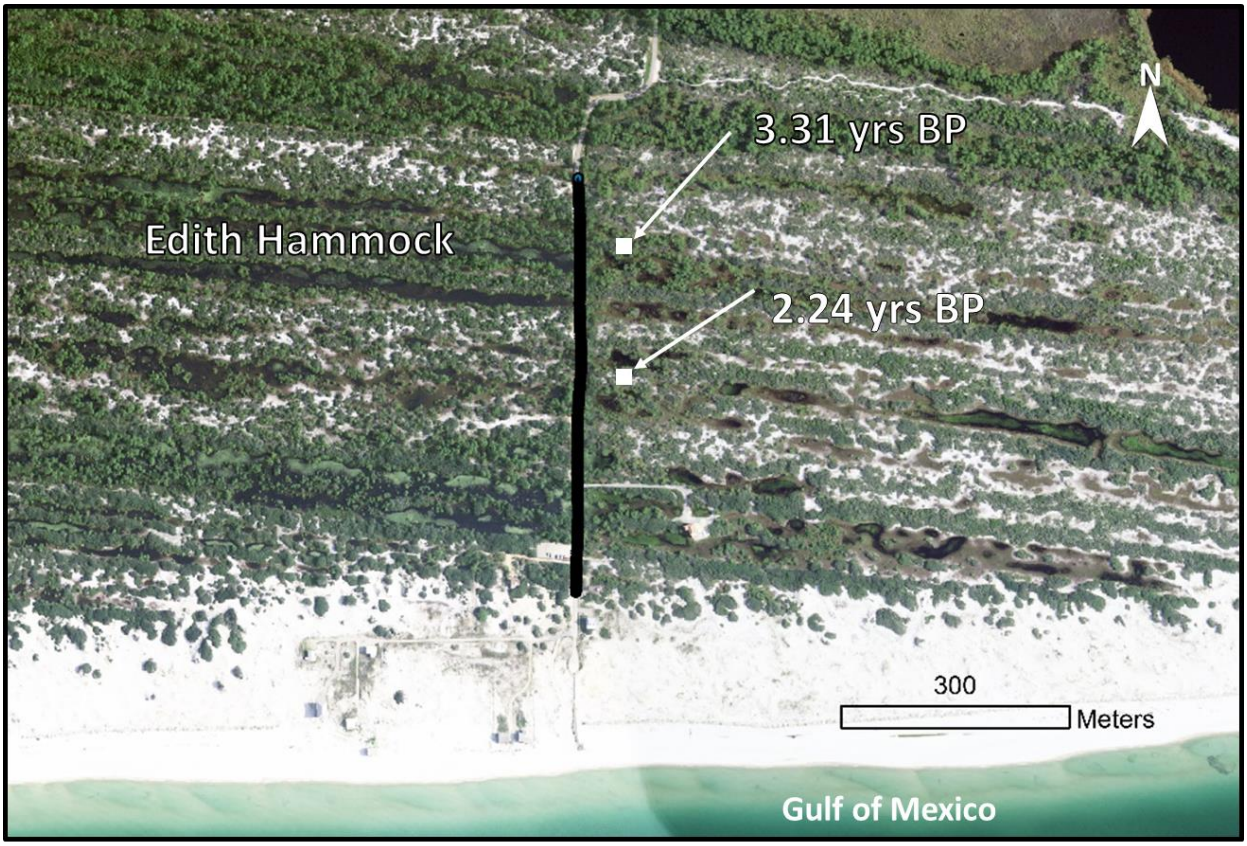

Figure 13. The Mobile St. GPR profile path in the Edith Hammock Shoreline. Profile acquisition was obtained along the eastern margin of Mobile St. Imagery obtained from 2014 USDA NAIP dataset.

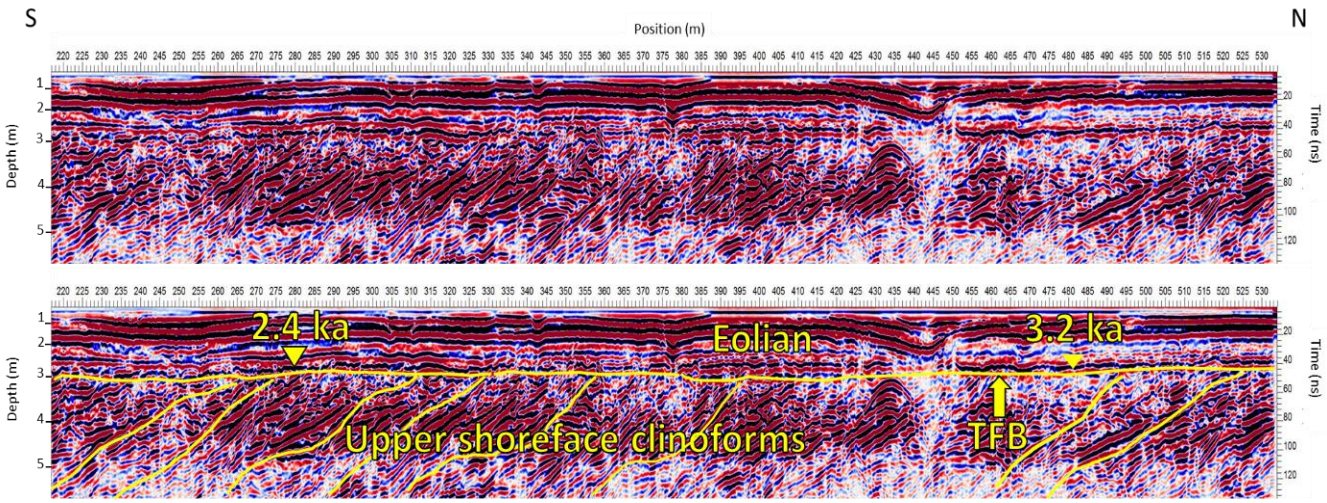

Figure 14. (A) Uninterpreted and interpreted 310 m section of the Mobile Street GPR profile. The topset-foreset break and the general dips of seaward-dipping shoreface clinoform foresets are highlighted with yellow lines on the bottom image.

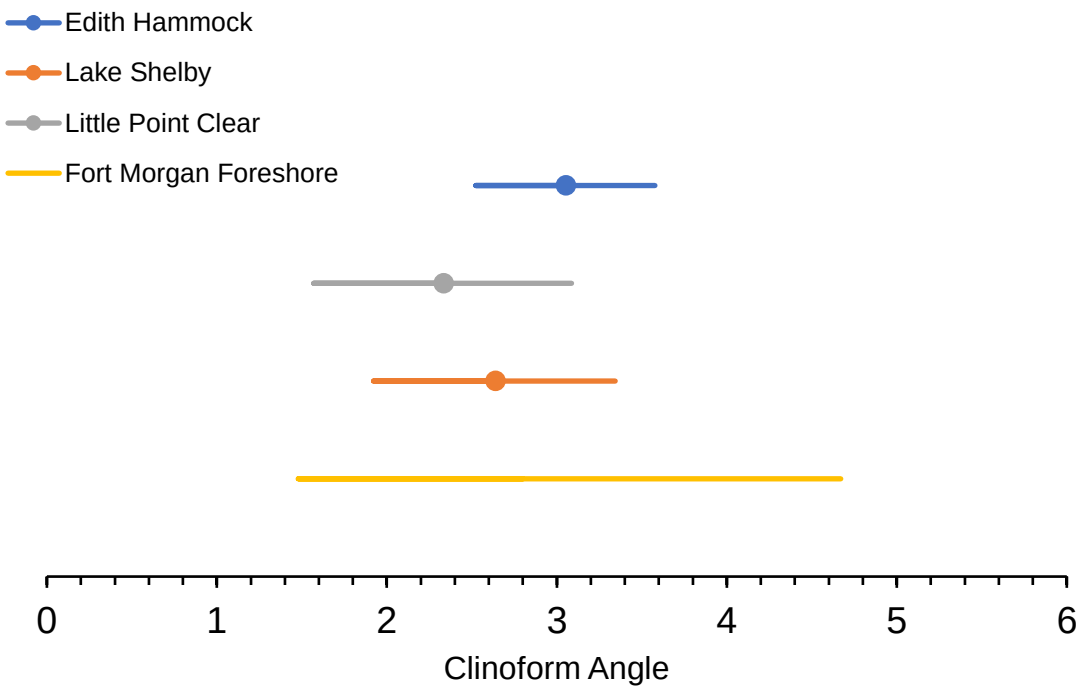

Figure 15. Measured clinoform angles from GPR profiles used in the present study and from the modern Fort Morgan shoreface. Mean values for the Lake Shelby, Little Point Clear, and Edith Hammock beach-ridge plains are indicated by a circle and one standard deviation from the mean angle of each profile is represented by the line. Mean and standard deviation values are calculated from 10 measured clinoforms from each GPR profile location. Modern shoreface values for Fort Morgan were extracted from Rodriguez and Meyer (2006), who obtained them from Douglass (2001).

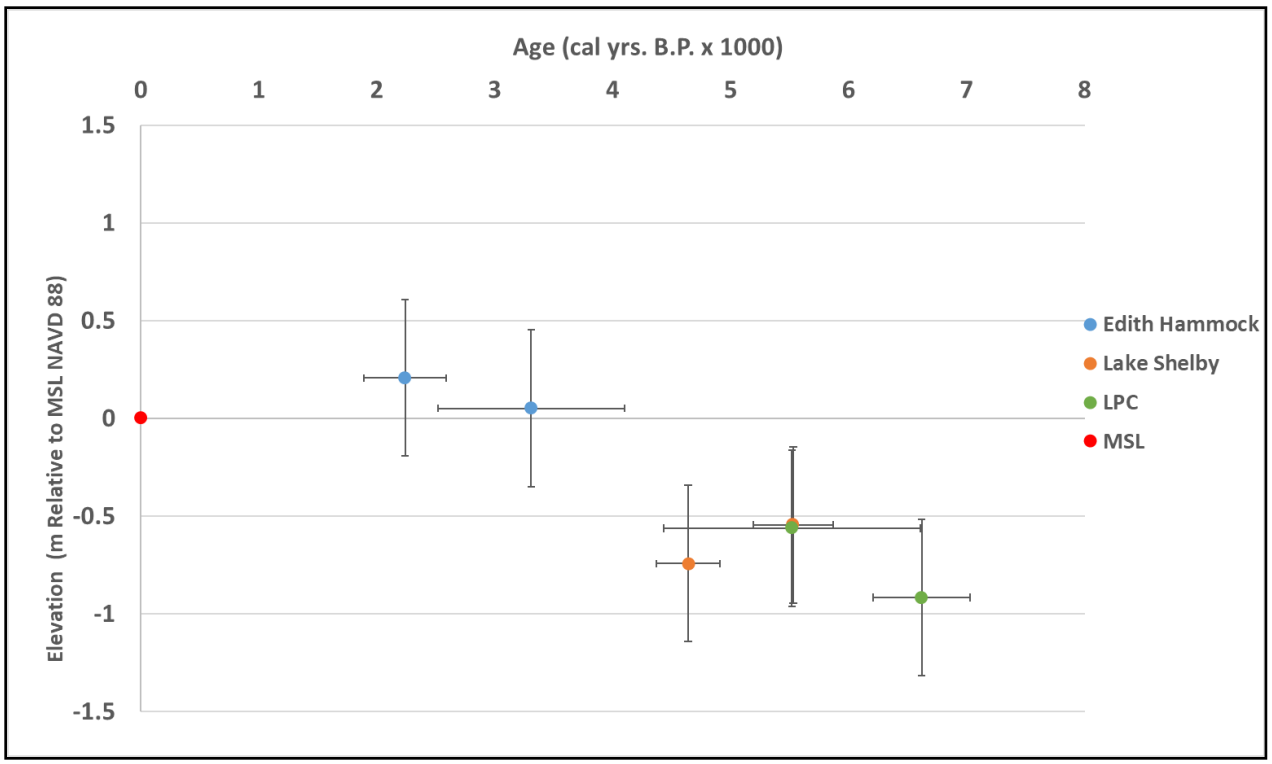

Figure 16. Middle to late Holocene sea-level positions calculated for this study. The vertical error in this study is 0.43 m. The OSL age error was adopted from Blum et al. (2003) and was applied independently for each sea-level indicator.

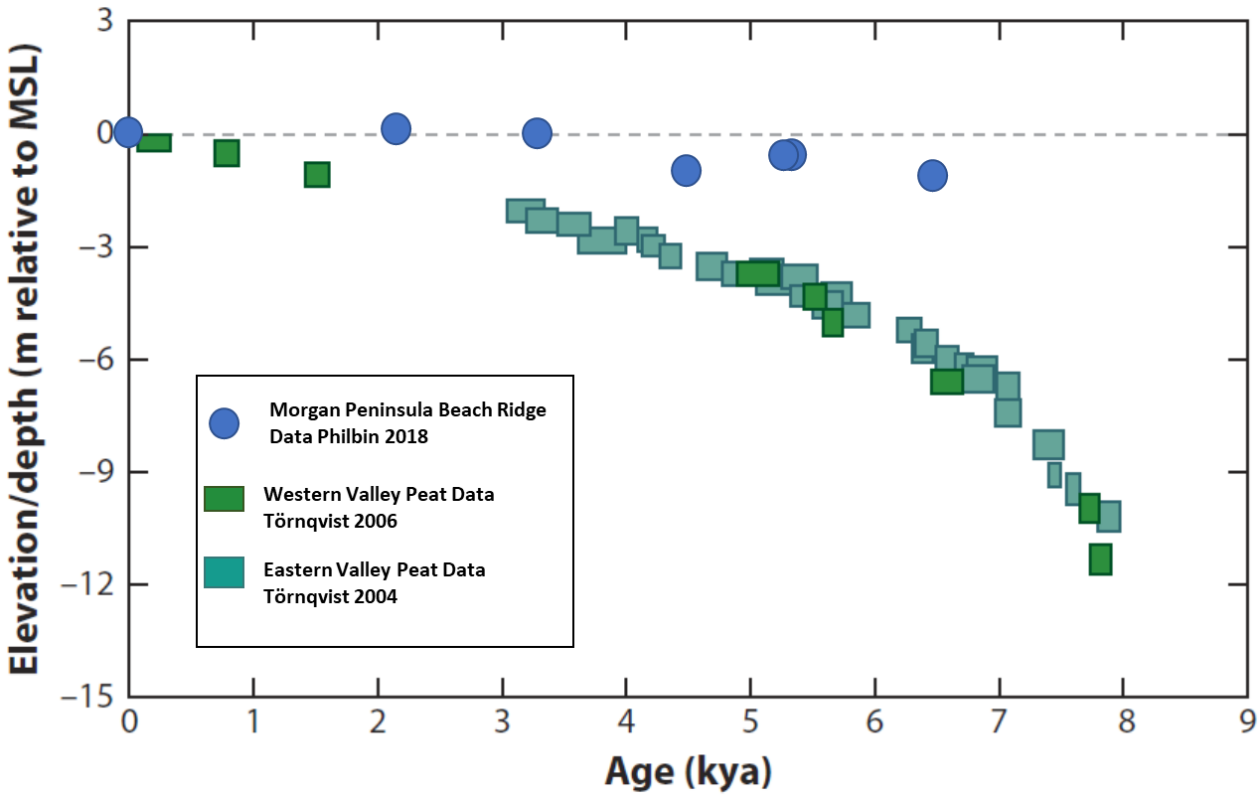

Figure 17. Morgan Peninsula beach-ridge plain sea-level indicators compared with sea-level positions reconstructed for the Mississippi delta region from basal peats. Adapted from Blum et al. (2008)

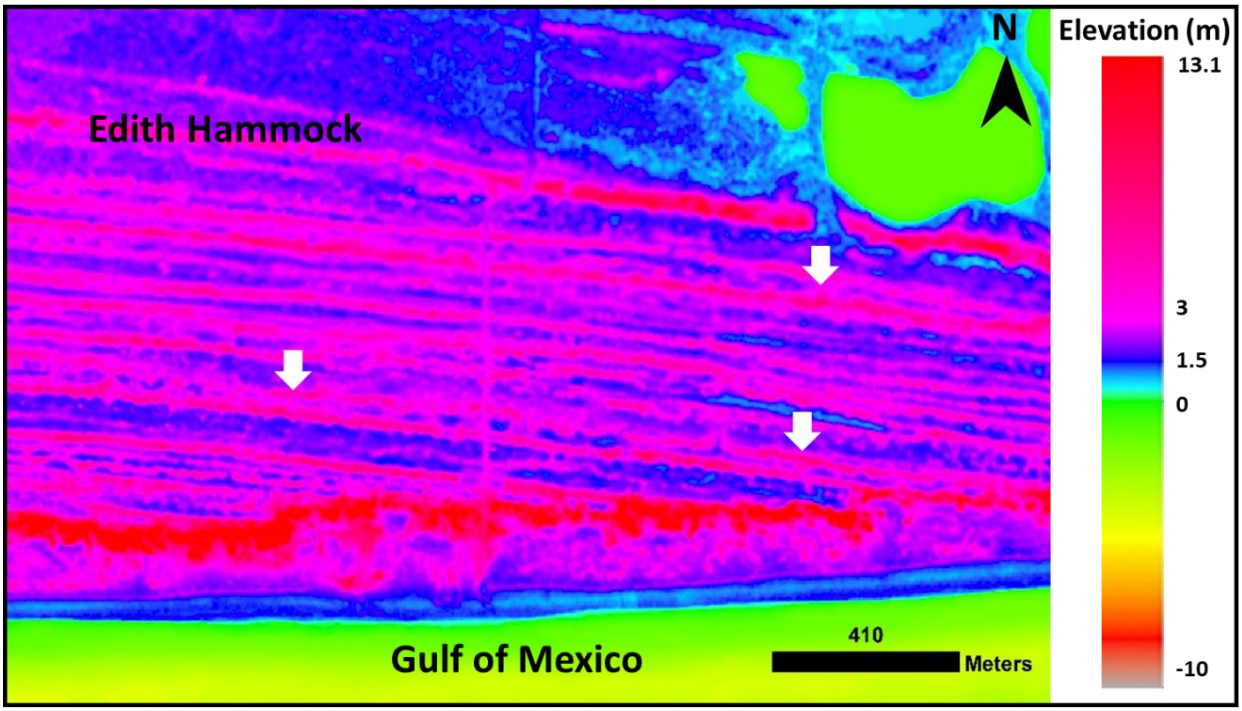

Figure 18. LiDAR DEM for the Edith Hammock beach-ridge plain with white arrows that point to merging and diverging of individual beach-ridge trends (data from the USGS, 2014).

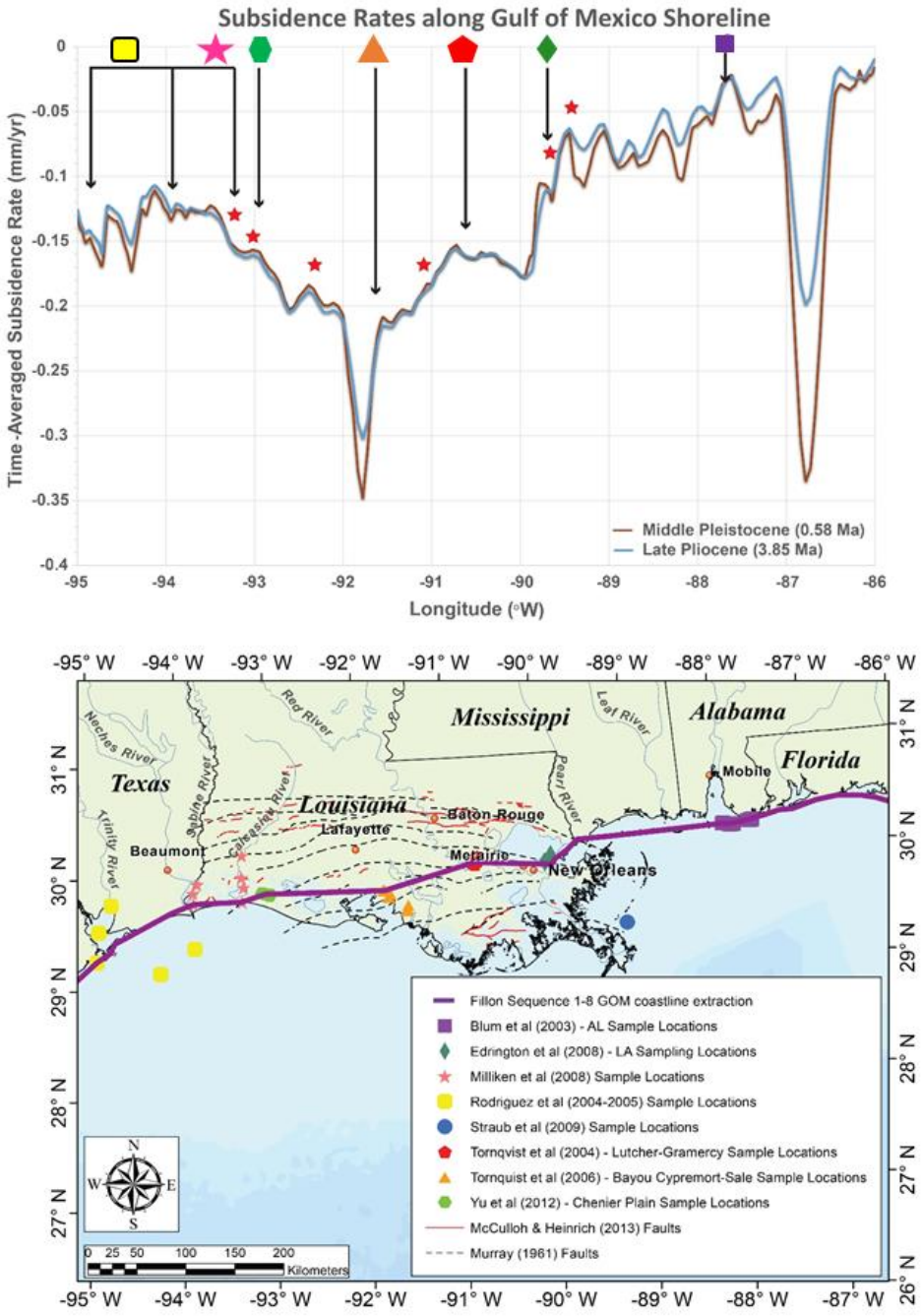

Figure 19. Along-strike profile of deep-seated subsidence rates along the northern Gulf of Mexico shoreline (upper plot), extracted to cross through locations where studies of Holocene sea-level change had been conducted (lower map) from Frederick et al. (2019). The red stars on the upper plot indicate where the profile crossed growth faults. The other symbols correspond to the corresponding studies in the lower map. Studies of sea-level change that have relied on basal peats have been located within the Mississippi delta "bowl" of subsidence, whereas Morgan Peninsula beach-ridge plains are located in a part of the coastline where long-term subsidence rates are negligible.

9. Tables

Location	Sea-Level Indicator	Indicative Meaning	Chronological control	Interpreted Trends	Reference
Florida panhanlde	beach ridge morphology and grain size	maximum SL	none	middle and late Holocene highstand	Tanner, Stapor etc.
Alabama coast	beach ridge morphology and grain size	maximum SL	OSL ages on beach deposits	oscillations since middle Holocene	Blum et al. (2002; 2003)
Alabama coast	ground-penetrating radar facies	uncertain	radiocarbon ages on shells within beach deposits	continual submergence	Rodriguez and Meyer (2006)
Mississippi delta	interbedded peats	minimum SL	radiocarbon ages on peats and shells	continual submergence	Frazier (1974)
Mississippi delta	interbedded peats	minimum SL	radiocarbon ages on peats	continual submergence	Kulp (2000)
Mississippi delta	barrier island sand	uncertain	radiocarbon ages on shells within beach deposits	middle Holocene highstand and subsequent SL fall	Stapor and Stone (2004)
Mississippi delta	basal peats	water table	radiocarbon ages on basal peats	continual submergence	Tornqvist et al. (2004; 2006)
Louisiana Chenier Plain	basal peats	water table	radiocarbon ages on basal peats	continual submergence	Yu et al. (2012)
East Texas coast and shelf	interbedded peats and shells	minimum SL	radiocarbon ages on peats and shells	continual submergence	Curray (1960)
East Texas coast and shelf	shells	minimum SL	radiocarbon ages on shells	stepwise submergence	earlier Rice work
East Texas coast and shelf	interbedded peats and shells	minimum SL	radiocarbon ages on peats and shells	continual submergence	Milliken et al. (2008)
Central Texas coast	coastal landforms	maximum SL	radiocarbon ages on shells	middle and late Holocene highstands	Morton et al. (2000)
Central Texas coast	interbedded peats and forams	minimum SL	radiocarbon ages on forams	middle Holocene highstand	Blum et al. (2001)
Central to South Texas coast	algal matts in coastal ponds	maximum SL	radiocarbon ages on algal matts	continual submergence	Simms et al.

Table 1: List of published studies of Holocene sea-level change for the northern Gulf of Mexico, and the sea-level indicators used.